

RESPONSES TO THE EDITOR'S COMMENTS (*in italics*)

Topic Editor Decision: Publish subject to minor revisions (review by editor) (31 Jul 2020) by [Joanne Williams](#)

Comments to the Author:

Dear authors,

Thank-you for your revised manuscript, and response to the reviews. There are a few minor issues remaining, as follows.

Table 1: please be consistent in usage of Ku-band (ideally \$K_u\$)

Corrected

Table 1: sea-state bias (spelling)

Corrected

line 159: western Mediterranean Sea

Corrected

line 167: "Senetosa is operating"? The place can't operate it. Perhaps "Since 1998 a calibration site has operated near the Senetosa lighthouse, with support from..."?

Modified as suggested

line 176: You could tidy this a little, eg "M4/M5 as a few cm apart, sheltered from the northwest-ward wind, whilst M3 is a 1.7km eastward, more exposed to open-sea conditions. "

Modified as suggested

Fig 1: Ensure the copyright is correctly handled for the Google earth image - See https://www.ocean-science.net/for_authors/manuscript_preparation.html

[OK](#)

line 210: Outliers are omitted in computing the regression line.

Corrected

line 245, 250 (and check elsewhere): "Figure 4 shows..." or "as shown in Fig. 4"

Corrected

line 255: Grammar. I suggest: "In coastal areas, precision of sea surface height from altimetry is limited by inaccuracies in some of the applied geophysical corrections (including sea state bias, wet tropospheric correction, dynamical atmospheric correction and ocean tides) and from the distorted

shape of the radar waveforms as the satellite approaches land (Vignudelli et al., 2011 and Cipollini et al., 2018).

Modified as suggested

line 260: Bit vague. I think you mean that data that is not flagged can still have errors due to coastal proximity?

Modified

line 265/269 : Try not to switch tense. examined?

Modified

line 269: reads like $d(ssb)/d(\text{distance to coast})$. I suggest "We plotted trends in geophysical correction against distance to the coast, for sea-state bias..."

Modified as suggested

Fig 6b is unnecessary. Suggest line 329 becomes "We resampled the along-track sea-level records keeping only the 80% of data common to all along track positions at a given time."

Fig.6b has been deleted

Line 329 modified as suggested

line 333 cut "then"

Done

Fig 7: as a general rule for color-vision accessibility, avoid red vs green lines. Replot if possible, however it does not significantly affect the message of this figure so I don't insist on it. However in Fig 20 it does matter, please replot.

We have not modified the figures except Fig.20 which has been redrawn (blue instead of red)

line 383: full stop.

Done

line 515: cut "well"

Done

Fig 10: would be more intuitive rotated to align with the map. However it is not essential.

In effect, this is not essential

Fig 12: It would have been good to see the altimetry results alongside here.

It will be the purpose of another paper in preparation where we compare tide gauge records with coastal SLA time series at Senetosa and several other sites

line 595: "it is very unlikely that wave set up explains the reported coastal sea level trend."

Modified as suggested

lines 604-715: The argument in this section is rambling and hard to follow. It needs tidying up and probably condensing. You can simplify a lot of sentences.

As I understand your argument ...

Could waves explain the SLA trends approaching the coast? SWH at a nearby ERA grid point has little correlation with SLA at 15km, but has some correlation with SLA at the coast, Fig15 & Fig 16a. One mechanism for waves to affect the altimetry corrections is via ssb. SWH at the ERA grid point does not correlate well with ssb near the coast (Fig 16b & Fig 17). So it is possible the wrong ssb is used as an altimetry correction near the coast (slightly better in ALES). Therefore though the waves do correlate with SLA, it's not via ssb, so it's not causal. So despite fig 16a, the argument in the first part of 6.1 still holds? You say you have eliminated waves as the explanation.

However in section 6.2 we learn that the winds are highly seasonal and affect the local currents. Seasonal changes in wind direction would directly affect the local SWH, since sometimes the coast will be sheltered. More localised wind and wave information would be very helpful here. Otherwise I think you can only say that there is no strong evidence for waves and ssb causing the trend in SLA.

If I've got this right it's after a lot of unpicking. Please clarify. If I've got it wrong, then this *really* needs clarifying.

It seems that our text was unclear because the above comment is exactly the opposite of what we wanted to say, ie., that the correlation between waves and SLA is do to the wrong SSB. Schematically:

1) SLA without SSB correction is always correlated with SWH (the SSB phenomenon is a function that is directly proportional to SWH. It is THERE until we remove it with a correction)

2) If we apply the SSB correction correctly, we decrease the correlation between SLA and SWH

3) If the SSB correction is wrong, the correlation remains. This is what we see very close to the coast.

The confusion comes from the fact that, although we are focusing on the explanation that the ssb correction is not being effective very very close to the coast, we still (during the section) keep open the possible explanation that the correlation between SWH and SLA is physical ("This clearly suggests that computed SLAs are impacted by waves in the last few km to the coast on a broad range of time scales").

We have modified the text of the revised version to make the argumentation clearer. We have also added a short introduction to explain what we want to demonstrate.

specifics from this section:
line 604: cut "However"

Done

line 609: we consider sea-level anomalies...

Corrected

line 610: cut "mesh"

Done

line 610: Please indicate the position of the ERA5 grid point you use on one of the maps. ERA5 grid spacing is about 30km so it matters. It is a pity you don't have anything finer resolution here.

We have added a sentence in the text indicating the position of the closest grid mesh to Senetosa

line 638-640: No. Fig 16a doesn't show the interannual correlation, because it is swamped by the seasonal signal. You'll have to replot this or at least recalculate R after filtering the seasonal out.

The correlation is mostly based on the seasonal signal but as the amplitude of the latter varies with time in the same way in both time series, this indicates that the correlation also holds at interannual time scale

line 693: The correlations are really rather weak here. Suggest "As expected, ssb is correlated with wave height away from the coast, but..." It is difficult to see any relationship from the figure. Replot with the orange ssb curves on a different scale (eg use a right-hand axes).

Modified as suggested

line 699: You haven't calculated significance. Rephrase.

Modified as suggested

lines 729-733: could condense this.

Done

Fig 18 & 19: could be combined. And why zonal only? You need the meridional component too to give the along-shore current.

Only the zonal components shows some trend. More investigation is on going using the MARS3D model around Senetosa and this will be the subject of another paper in preparation.

Please indicate 15 km along-track distance on at least one map.

Done in the text

Although you can't derive a trend from the MARS3d model, and it's fair enough to pass on the coastal

oceanography to another study, it would be very helpful to do a seasonal comparison, perhaps plot a different season in Fig 18.

See above comment

line 832: cut "elongated"

Done

line 834: an indication

Corrected

You have not met all requirements in

https://www.ocean-science.net/for_authors/manuscript_preparation.html

Please attend particularly to data referencing, but check through other requirements as well. Don't rely on the typesetter to find them!

The MARS3d model, ERA5 data (they have a standard format statement required), altimetry data all need correct acknowledgement and statement of where to access the data. This should be in a Data Availability section.

A Data availability section added

All modifications of the 3rd revised version of the manuscript are highlighted in blue

1
2
3
4
5
6
7
8
9
10
11
12
13
14
15
16
17
18
19
20
21
22
23
24
25
26
27
28
29
30
31
32
33
34
35
36
37
38
39
40
41
42
43
44
45
46
47
48

Coastal Sea Level rise at Senetosa (Corsica) during the Jason altimetry missions

Yvan Gouzenes¹, Fabien Léger¹, Anny Cazenave^{1,2}, Florence Birol¹, Pascal Bonnefond³,
Marcello Passaro⁴, Fernando Nino¹, Rafael Almar¹, Olivier Laurain⁵, Christian Schwatke⁴,
Jean-François Legeais⁶ and Jérôme Benveniste⁷

1. LEGOS, Toulouse; 2. ISSI, Bern; 3. Observatoire de Paris-SYRTE, Paris ; 4. TUM,
Munich; 5. Observatoire de la Côte d'Azur-Géoazur, Sophia-Antipolis; 6. CLS, Ramonville
St Agne; 7. ESA-ESRIN, Frascati.

3rd Revision
~~5²~~ August 2020
Corrections highlighted in blue

Corresponding author: Anny Cazenave (anny.cazenave@legos.obs-mip.fr)

49
50
51
52

53 **Abstract**

54 In the context of the ESA Climate Change Initiative project, we are engaged in a regional
55 reprocessing of high-resolution (20 Hz) altimetry data of the classical missions in a number of
56 world's coastal zones. It is done using the ALES (Adaptive Leading Edge Subwaveform)
57 retracker combined with the X-TRACK system dedicated to improve geophysical corrections
58 at the coast. Using the Jason-1&2 satellite data, high-resolution, along-track sea level time
59 series have been generated and coastal sea level trends have been computed over a 14-year
60 time span (from July 2002 to June 2016). In this paper, we focus on a particular coastal site
61 where the Jason track crosses land, Senetosa, located south of Corsica in the Mediterranean
62 Sea, for two reasons: (1) the rate of sea level rise estimated in this project increases significantly
63 in the last 4-5 km to the coast, compared to what is observed further offshore, and (2)
64 Senetosa is the calibration site for the Topex/Poseidon and Jason altimetry missions,
65 equipped for that purpose with in situ instrumentation, in particular tide gauges and GNSS
66 antennas. A careful examination of all the potential errors that could explain the increased
67 rate of sea level rise close to the coast (e.g., spurious trends in the geophysical corrections,
68 imperfect intermission bias estimate, decrease of valid data close to the coast and errors in
69 waveform retracking) has been carried out, but none of these effects appear able to explain
70 the trend increase. We further explored the possibility it results from real physical processes.
71 Change in wave conditions was investigated but wave set up was excluded as a potential
72 contributor because of too small magnitude and too localized in the immediate vicinity of
73 the shoreline. Preliminary model-based investigation about the contribution of coastal currents
74 indicates that it could be a plausible explanation of the observed change in sea level trend
75 close to the coast.

76

77 **1. Introduction**

78 Since the early 1990s, satellite altimetry provides invaluable observations of the global mean
79 sea level and its regional variability. In the recent years, this data set has generated an
80 abundant literature on the processes causing sea level change at global and regional scales, as
81 well as on closure of the sea level budget (e.g., Church et al., 2013, Stammer et al., 2013,
82 Dieng et al., 2017, Nerem et al., 2018, WCRP, 2018, SROCC, 2019). In addition to the global
83 mean rise and superimposed regional trends, changes in small scale processes such as local
84 atmospheric effects, baroclinic instabilities, coastal trapped waves, shelf currents, waves,
85 fresh water input from rivers in estuaries, can substantially modify the rate of sea level change
86 at the coast compared to open sea regions (Woodworth et al., 2019, Melet et al., 2018,
87 Piecuch et al., 2018, Dodet et al., 2019, Durand et al., 2019). In addition, ground subsidence
88 may amplify the rate of sea level change at the coast (Woppelmann and Marcos, 2016). In
89 terms of societal impacts, what really matters in the coastal zone is indeed the sum of the
90 global mean sea level rise plus the regional trends and the local processes.

91 Up to recently, due to land contamination of radar echoes and less precise geophysical
92 corrections, classical altimetry did not provide reliable sea level data in a band of 10-15 km
93 along coastlines. However different studies have shown that using adapted reprocessing of
94 altimetry measurements and improving geophysical corrections allows retrieving a large
95 amount of valid sea level close to the coast (e.g., Cipollini et al., 2018, Passaro et al., 2015,
96 Marti et al., 2019). In addition, despite having a much higher noise level than the classical 1
97 Hz altimetry data, high-resolution 20 Hz measurements allow to recover more information on
98 coastal sea level variations (Birol and Delebecque, 2014, Leger et al., 2019).

99 In the context of the Climate Change Initiative (CCI) project of the European Space
100 Agency (ESA), we have initiated a reprocessing of high-resolution (20 Hz) altimetry data of
101 the Jason-1 and Jason-2 missions along coastal zones of Western Africa, Northern Europe and
102 Mediterranean Sea. The ALES (Adaptive Leading Edge Subwaveform) retracker (Passaro et
103 al., 2014) was applied to estimate the satellite-sea surface distance (called range) which was
104 further combined with the X-TRACK processing chain dedicated to improve geophysical
105 corrections at the coast (Birol et al., 2017). This allowed us to derive along-track sea level
106 anomaly (SLA) time series (Leger et al., 2019) from which coastal sea level trends were
107 estimated. Results show that in a number of sites, coastal sea level rates computed over a 14-
108 year time span (2002-2016) significantly deviate from the open ocean rate within 5 km to the
109 coast (Marti et al., 2019).

110

111 In the present study, we focus on a particular site, Senetosa, located southern Corsica in the
 112 Mediterranean Sea ($41^{\circ} 33'N$, $8^{\circ}48'E$), for two reasons: (1) in this region, the computed rate
 113 of sea level rise increases significantly in the last 3-5 km to the coast, and (2) there is a
 114 Jason satellite track that crosses land at Senetosa, a calibration site for altimetry missions
 115 chosen since the launch of the Topex/Poseidon mission in 1992 and equipped for that purpose
 116 with in situ instrumentation, in particular tide gauges and GNSS antennas (Bonfond et al.,
 117 2019). This calibration site provides an independent reference to explore the near-shelf signal
 118 observed in altimetry data.

119

120 2. Data and method

121 As presented in detail in Marti et al. (2019) and Léger et al. (2019), here we use the regional
 122 X-TRACK/ALES along-track 20 Hz SLA data derived from Jason-1 and Jason-2 missions
 123 (DOI: 10.5270/esa-sl_cci-xtrack_ales_sla-200201_201610-v1.0-201910). This product is
 124 based on new ranges and new sea state bias corrections estimated using the ALES retracker
 125 (see details on the retracking methodology in Passaro et al., 2014), and further combined with
 126 the X-TRACK software developed at CTOH (Center of Topography of the Ocean and the
 127 Hydrosphere) at LEGOS (Laboratoire d'Études en Géophysique et Océanographie Spatiales).
 128 The new X-TRACK/ALES processing system first downloads from the altimetry database
 129 hosted by the French National Observations Service for altimetry called CTOH
 130 (<http://ctoh.legos.obs-mip.fr/>), all parameters needed to compute the sea level anomaly (orbit
 131 solution, altimeter ranges, instrumental, environmental and geophysical corrections). These
 132 parameters come from the Geophysical Data Records (GDRs) data sets distributed by the space
 133 agencies for the different altimetry missions. ALES range and SSB products come from TUM.
 134 Additional geophysical corrections are provided by the RADS altimeter database
 135 (<http://rads.tudelft.nl/rads/rads.shtml>) and the University of Porto (for the GPD+ wet
 136 tropospheric correction, Fernandes et al., 2015). Concerning the geophysical corrections, we
 137 used the standards defined in the ESA CCI sea level project (<http://www.esa-sealevel-cci.org/>).
 138 These are summarized in Table 1.

139

Parameter	Source	Jason-1 / Jason-2
Altitude	GDR	Altitude of satellite
Range	ALES/TUM	20 Hz Ku band ALES corrected altimeter range (Passaro et al. 2014)

Sigma0	ALES/TUM	20 Hz Ku band ALES altimeter sigma0 (Passaro et al. 2014)
Ionosphere	GDR	From dual-frequency altimeter range measurement
Dry troposphere	GDR	From ECMWF model
Wet troposphere	University of Porto	GPD+ correction (Fernandes et al. 2015)
Sea-state bias	ALES/TUM	Sea-state bias correction in Ku band, ALES retracking (Passaro et al. 2018)
Solid tides	RADS	From tide potential model (Cartwright and Taylor 1971, Cartwright and Eden 1973)
Pole tides	GDR	From Wahr 1985
Loading effect	RADS	From FES 2014 (Carrere et al. 2012)
Atmospheric correction	RADS	From MOG2D-G (Carrere and Lyard 2003) + inverse barometer
Ocean tide	RADS	From FES 2014 (Carrere et al. 2012)

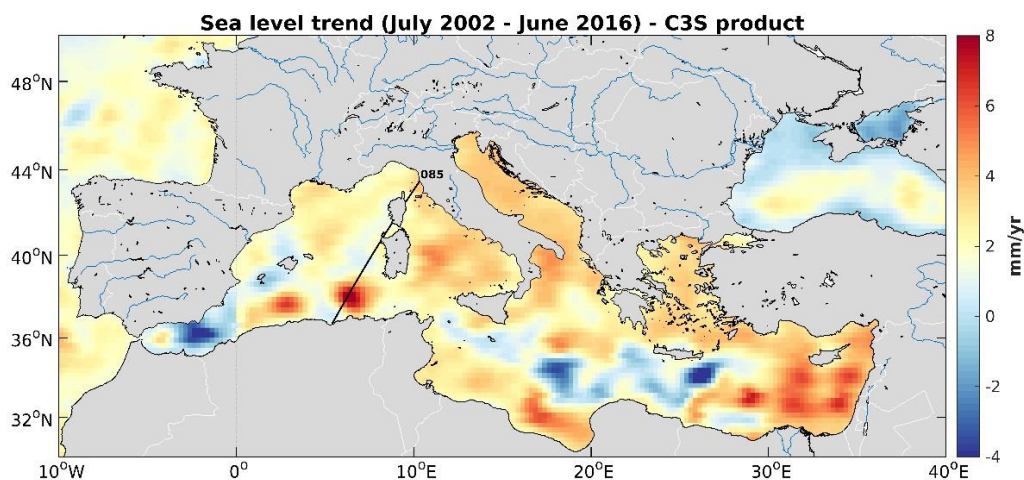
140

141 *Table 1: List of altimetry parameters and geophysical corrections used in the computation of the*
142 *coastal sea level products.*

143

144 A dedicated editing strategy was further applied to eliminate noisy data. For each orbit cycle, the
145 temporal behavior of each geophysical correction was analyzed along the satellite track. Abrupt
146 changes were considered as spurious and removed (Birol et al., 2017). This strategy has proved to
147 be very efficient in recovering a significant amount of valid altimeter measurements that were
148 otherwise flagged in the standard GDR products (Jebri et al., 2016). In a second step, all corrections
149 were recomputed at the 20-Hz high-rate using only the valid data, through interpolation/extrapolation
150 method. The sea level data of each cycle were further projected onto fixed points along a nominal
151 ground track and converted into SLAs by subtracting a reference mean sea surface. At this stage of
152 the processing, a regional dataset of SLA time series with a spatio-temporal resolution of 10 days
153 and 20Hz (~0.3 km) was produced for each Jason mission. To obtain a single multi-mission product,
154 an inter-mission bias was estimated and removed. This was done at regional level by computing the

155 mean sea level differences between the two missions over their overlapping period (calibration
156 phase). The resulting SLAs were further averaged on a monthly basis at every 20 Hz point and an
157 additional editing was performed to remove outliers (details in Marti et al., 2019).
158 In this study we focus on the section of Jason track 85 located off the southwestern coast of
159 Corsica island (**western Mediterranean Sea**) (see Fig. 1).
160



161

162

163 *Fig. 1: Location of the Jason track 85 crossing Corsica at the Senetosa site (black straight line).*
164 *The background maps shows sea level trends over 2002-2016, based on gridded altimetry data*
165 *from the Copernicus Climate Change Service (C3S)*

3. The Senetosa calibration site

166 Since 1998, a calibration site of the Topex/Poseidon and Jason missions has
 167 operated near the Senetosa lighthouse with support from CNES (Centre National
 168 d'Études Spatiales, France), NASA (National Aeronautics and Space Administration, USA)
 169 and the Observatoire de la Côte d'Azur (France). It is equipped with different in situ
 170 instrumentation, including weather stations, several tide gauges and GNSS antenna. Since
 171 1998, this calibration site has been widely used to validate the altimetry-based sea surface
 172 height data (Bonnetfond et al., 2003a,b, 2010, 2011). Fig.2 is a Google Earth image of the
 173 coast, showing the geographical configuration of the Senetosa calibration site, with the
 174 location of the tide gauges, the GNSS antenna and the Jason track. Three tide gauges were
 175 operating during our study period (M3, M4 and M5). M4 and M5, a few tens of cm apart,
 176 are located on the western part of the coastline sheltered from northwestward wind
 177 forcing. M3 at 1.7 km eastward of M4/M5 is more exposed to open sea conditions from the
 178 west.
 179

180 Vertical land motion time series are available from the GNSS reference receiver located close
 181 to the lighthouse (G0 reference marker in Fig.2). The tide gauges have been regularly leveled
 182 relatively to the G0 reference marker with no relative motion detected so far at the millimeter
 183 level over 10 years. Trends in sea level and vertical land motions derived from these
 184 instruments at Senetosa are discussed in section 5.

185



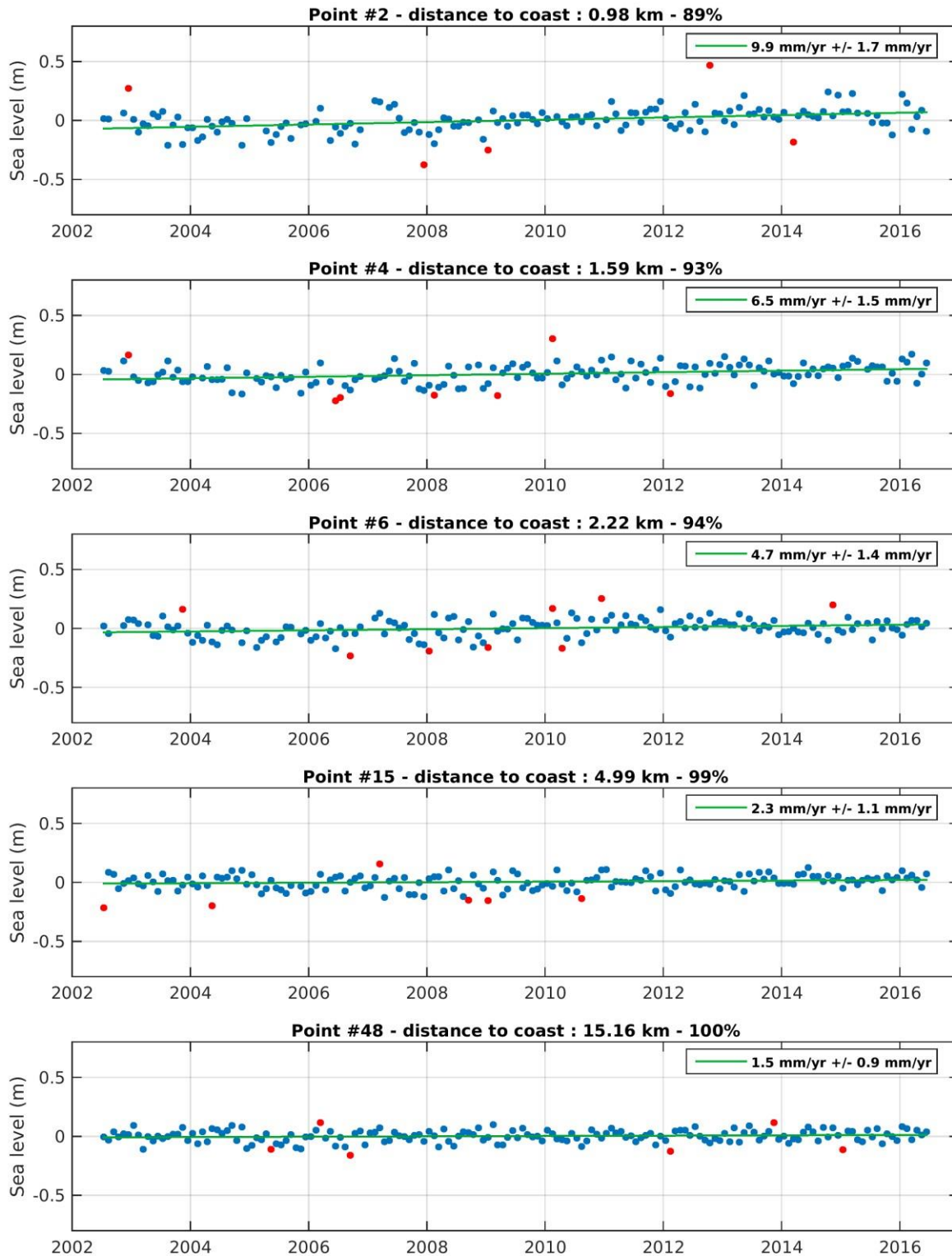
187
188 *Fig. 2: Google Earth image of the Senetosa calibration site. The two tide gauge sites (referred*
189 *as M4/M5 and M3) are shown by the red dots. The G0 reference marker (G0) is indicated by a*
190 *white square and the Jason ground track by the white straight line.*

191
192

193 **4. Analysis of the coastal sea level trends off Senetosa**

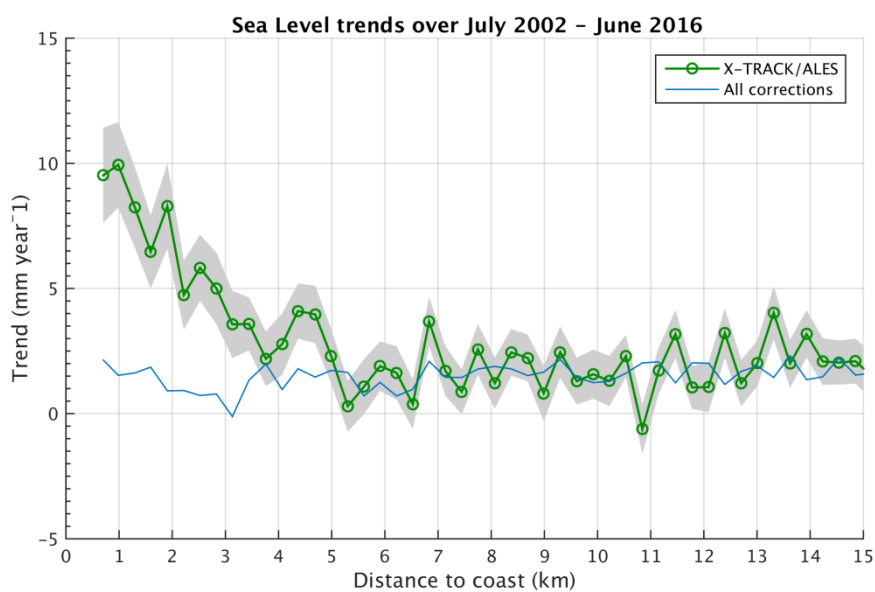
194 **4.1 Coastal sea level trends derived from altimetry data**

195 Following the data processing described above, we focus on monthly SLA time series sampled
196 at 20 Hz (~350 m in the along-track direction), from 15 km offshore to the coastline. Examples
197 of along-track SLA time series at coastal points, located at 1 km, 1.6 km, 2.2 km, 5 km and
198 15 km from the coast respectively, are shown in Fig.3.

199
200201
202
203

204 *Fig. 3: Examples of sea level anomalies time series for 20-Hz points located at different*
 205 *distances from the coast. The distance to coast, percentage of valid data and sea level trends*
 206 *are indicated on each plot. The green curve is the regression line adjusted to the data. The*
 207 *red points on the time series correspond to outliers detected using a simple 2-sigma filter*
 208 *(sigma corresponding to the SLA standard deviation). These are not considered to compute*
 209 *the regression line.*

210
211
212
213
214 For each 20 Hz point, we have then computed the regression line of the resulting SLA time
215 series and the associated standard deviation (1-sigma) based on the least squares fit, to estimate
216 sea level trends over the study time span. Fig.4 shows the corresponding along track sea level
217 trends as a function of distance to the coast (from 15 km offshore).



239
240 *Fig. 4: Altimetry-based sea level trends over July 2002-June 2016 around Senetosa as a*
241 *function of distance to the coast . Shaded area corresponds to trend uncertainty range. The*
242 *light blue curve is the sum of trends in individual corrections.*

243
244 **As shown in Fig.4,** beyond ~ 5 km from the coast towards the open sea, the trend over 2002-
245 2016 is relatively stable and on average on the order of 2-3 mm/yr. High frequency
246 oscillations around this value are observed between adjacent points but these are likely due to
247 noise and we note they are of the same order of magnitude or only slightly larger than the
248 standard deviation of trend estimates at each point (of ~1.5 mm/yr).

249 **As also shown in Fig.4,** we note an almost continuous increase in the trend in the last ~4-5 km
250 to coast. The corresponding trend uncertainties (standard deviation) are not significantly
251 larger than offshore (<2 mm/yr).

252

253 4.2 Robustness of the computed coastal trends

254 In coastal areas, precision of sea surface height from altimetry is limited by inaccuracies in
 255 some of the applied geophysical corrections (including sea-state bias, wet tropospheric
 256 correction, dynamical atmospheric correction and ocean tides) and from the distorted shape of
 257 the radar waveforms as the satellite approaches land (Vignudelli et al., 2011 and Cipollini et al.,
 258 2018).

259 The corresponding altimetry measurements are often discarded by the processing chains or
 260 flagged in the data sets as potentially erroneous, leading to low confidence sea level
 261 trend estimates near the coastline. These estimates can also be impacted by the lower
 262 percentage of valid data in the coastal zone, as well as by the uncertainty in the bias estimate
 263 between the two successive missions Jason-1 and Jason-2. In order to check whether the sea
 264 level trend increase close to the coast reported in section 4.1 is associated to one of these
 265 factors, each of them is independently examined.

266

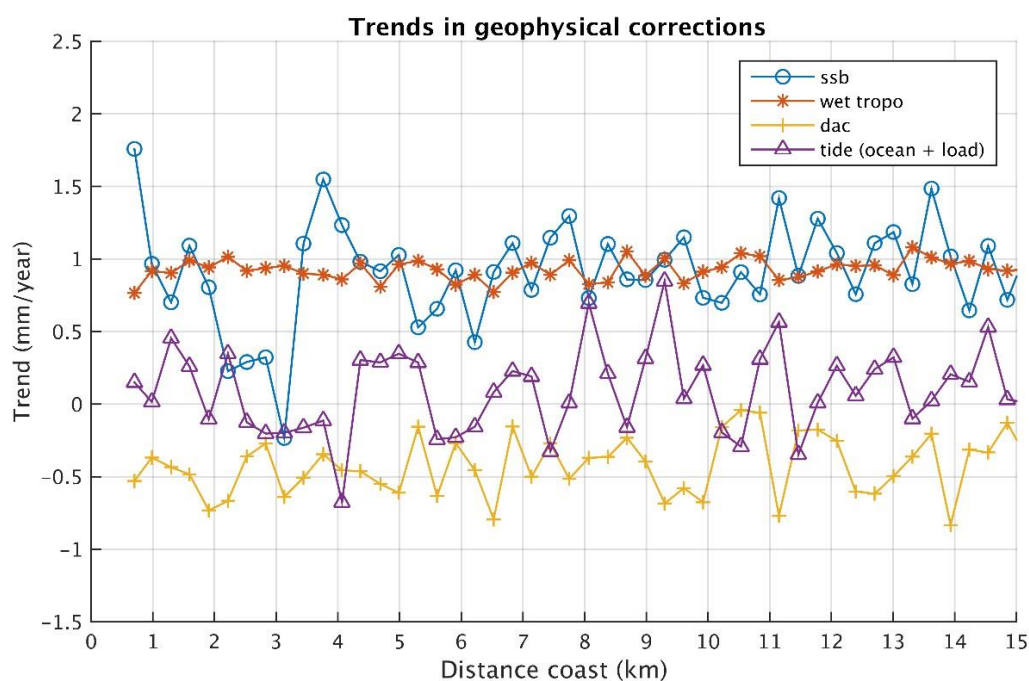
267 4.2.1 Coastal errors in the geophysical corrections

268 We first computed and plotted the geophysical correction trends against distance to the coast
 269 for the sea-state bias (ssb), wet atmospheric correction, atmospheric loading (called DAC-
 270 dynamic atmospheric correction-) and ocean and loading tide correction (Fig.5).

271

272

273



274

275
276
277
278

279 *Fig. 5: Trends in the geophysical corrections (sea state bias/ssb, wet tropospheric correction,*
280 *dynamic atmospheric correction/dac, ocean tide plus ocean loading tide) as a function of*
281 *distance to coast. Note that the vertical scale is different from Fig.4.*

282

283 Trends in the geophysical corrections are rather small and their amplitude in the range +/- 1
284 mm/yr, except for the ssb that shows a larger trend within 4 km to coast, but always less than
285 2 mm/yr. It is worth mentioning that the ssb is a function of significant wave height (SWH)
286 and backscatter coefficient (both related to wind speed). In the ALES retracking the ssb is
287 recomputed for each 20-Hz point. So a trend in ssb may be due to either a different behavior
288 of the SWH and wind speed at the coast, or to changes in backscatter properties.

289 The sum of these geophysical correction trends is plotted in Fig.4 (blue line). Even if the
290 geophysical corrections, and especially the ssb, are more uncertain close to the coast, Fig. 4
291 suggests that the continuous increase in the sea level trends observed in the last ~4 km to the
292 coast may not be due to trends in the geophysical corrections. It remains that the empirical
293 formulation used for the ssb correction may not be valid close to the coast where waves could
294 have a different behavior compared to the open sea. This will be discussed in section 6.1.

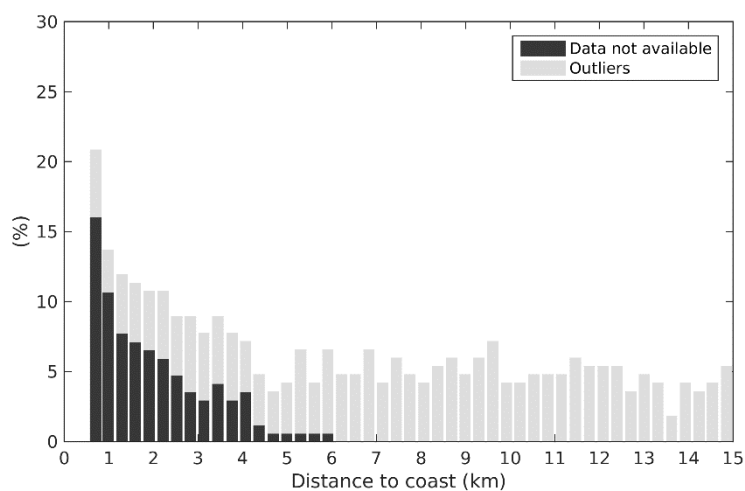
295

296 4.2.2 Coastal changes in the percentage of valid data

297 We next examined the possible impact on the trend estimation of the decrease in valid data in
298 the last 3-4 km to coast. The original percentage of valid data at each 20-Hz point decreases
299 with distance to the coast, as shown in Fig.6. We resampled the along-track sea-level records
300 keeping only the 80% of data common to all along track positions at a given time.

301

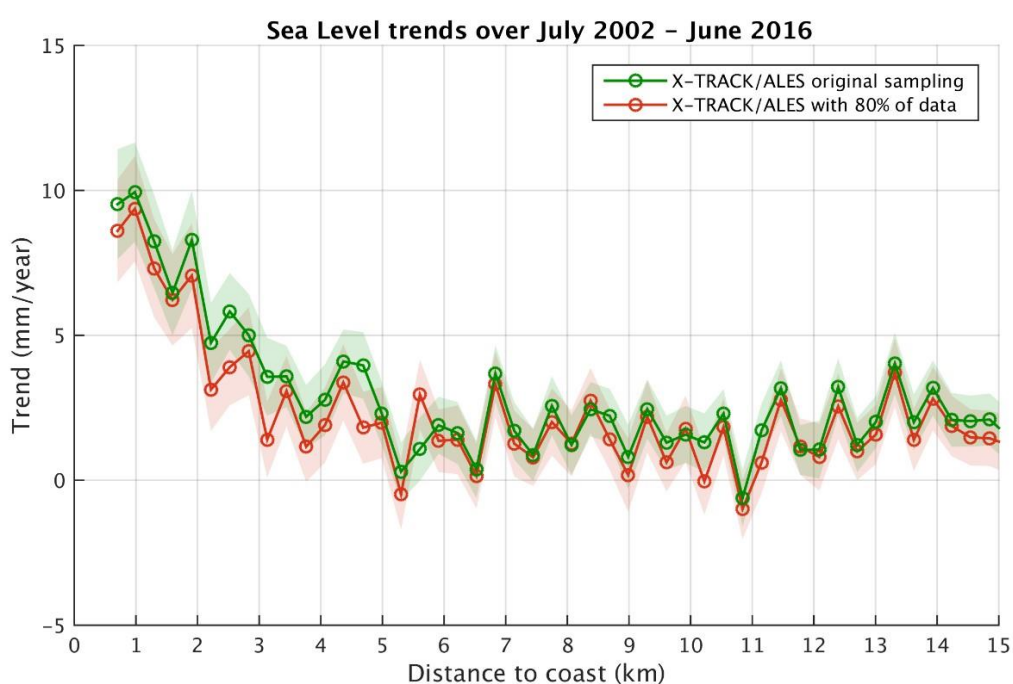
302



303
 304
 305
 306
 307
 308
 309
 310
 311
 312
 313
 314

Fig. 6: Percentage of missing points for the original data set.

The along-track sea level trends were recomputed with the new sampling (80% of the original data kept) (Fig.7). For comparison, in Fig.7 we superimpose the trends computed with the original sampling. Trends compare well in both cases. Even if the trend values are slightly lower in the band 0-5 km, keeping only 80% of the valid data does not change significantly the coastal trend behavior. We conclude that the lower amount of valid near-shore altimetry data does not explain the trend increase observed as the distance to the coast decreases.



315

316

317

318 *Fig. 7: Sea level trends as a function of distance to the coast with the original data set (green*
319 *curve) and new sampling (80% of original data kept; red curve).*

320

321

322 4.2.3 Effect of intermission bias estimation

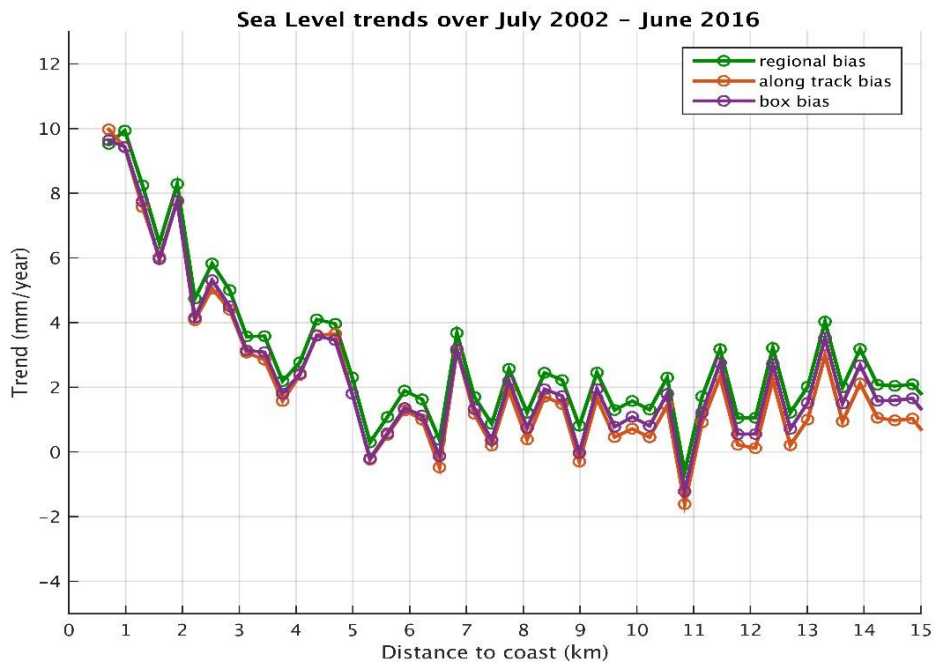
323 As discussed in detail in Marti et al. (2019), in the X-TRACK/ALES sea level product, the
324 bias applied to combine the Jason-1 and Jason-2 data in a single sea level time series was
325 estimated at a regional scale. In the case of our study region, it was estimated over the whole
326 Mediterranean Sea. In order to investigate a possible impact of this approach on the sea level
327 trend estimates, we tested other bias calculation methods. We first recomputed the
328 intermission bias along the Jason track 85 (using only measurements of this particular track).
329 In another test, the bias was computed from data included in a 1x1 degree box around the
330 Senetosa site. The sea level trends derived from the corresponding Jason-1 and Jason-2 time
331 series are shown in Fig. 8a for these two cases, superimposed to the regional bias case shown
332 in section 4.1. Here again, we can see that there is almost no difference between the results of
333 the three approaches, indicating that inadequate intermission bias estimate does not explain
334 the coastal trend increase. To complete these tests, we also recomputed SLA trends as a
335 function of distance to coast using as reference a local geoid computed for altimetry mission
336 calibration purposes (P. Bonnefond, personal communication). Fig.8b shows the geoid profile
337 together with the along-track mean sea surface computed with the altimetry data, as a function
338 of latitude. Both references compare well. Thus, as expected, exactly the same trend increase
339 behavior as a function of distance to coast is observed when the reference geoid is used
340 (figure not shown as it is similar to Fig.4). We conclude that the reference has no impact on
341 the computed trends.

342

343 (a)

344

345



346

347

348

349

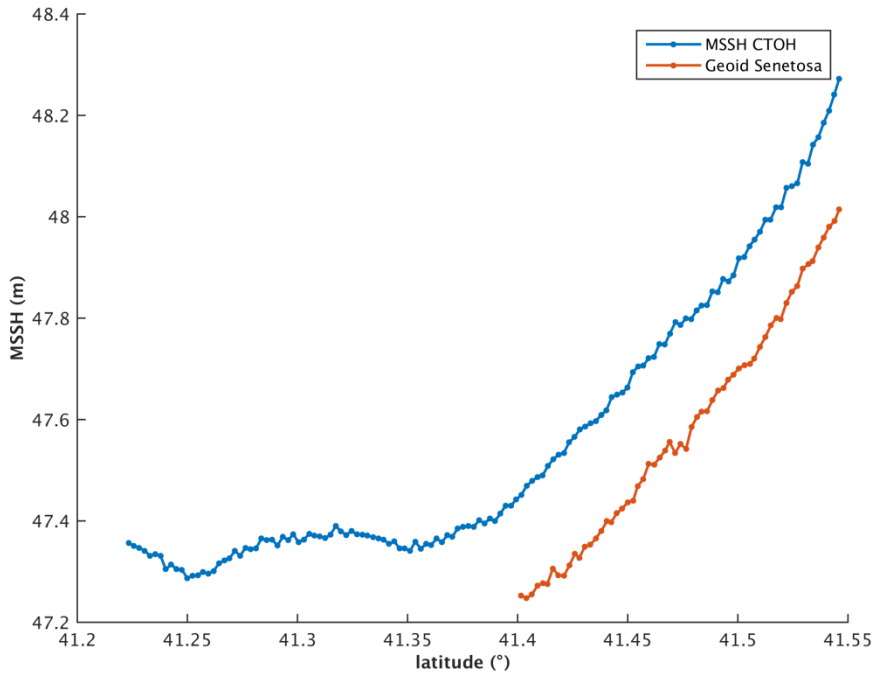
350

351 (b)

352

353

354



355
356
357

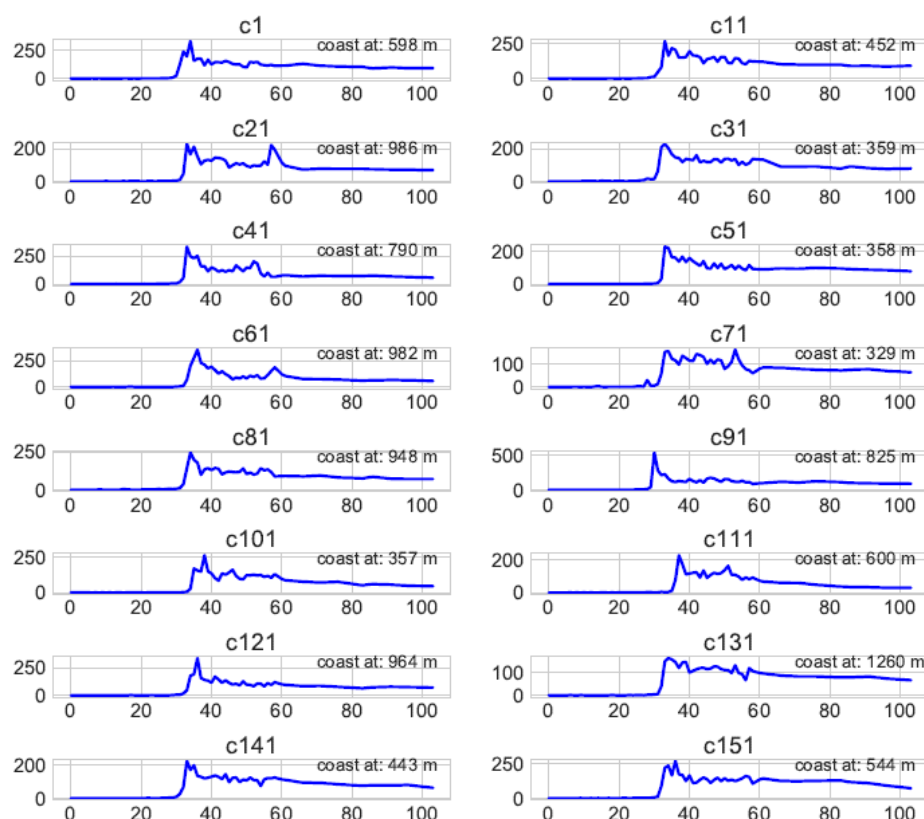
358 *Fig.8: (a) Sea level trends as a function of distance to the coast for three different intermission*
359 *bias estimates. (b) Geoid and altimetry-based along-track mean sea surface profiles as a*
360 *function of latitude.*

361
362

363 4.2.4 Coastal altimetry waveforms and range values near Senetosa

364 In another series of tests, we examined the shape of the radar waveforms at 20 Hz points as a
365 function of distance to coast, considering a few Jason cycles taken at random. An example is
366 shown in Fig. 9 for a point located between the coast and 2 km offshore. Fig.9 shows that at
367 the Senetosa site, the leading edge of the coastal radar echo is generally well defined,
368 suggesting that a robust determination of the range is possible very close to the coast.

369
370



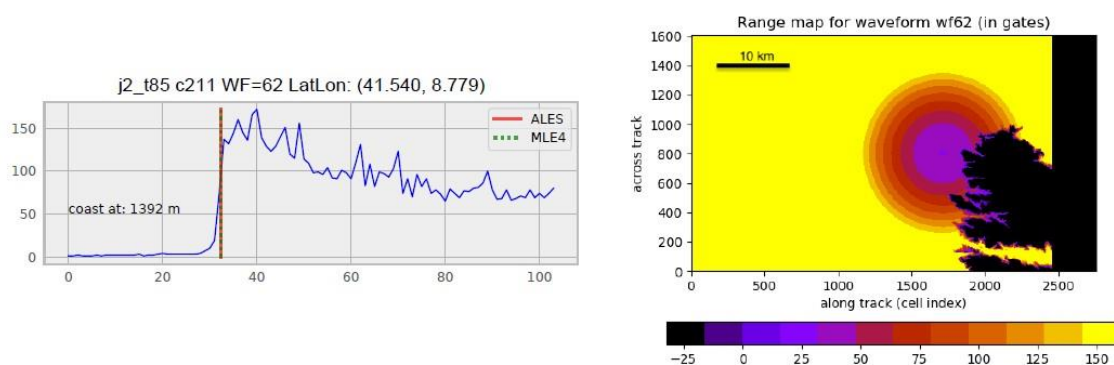
371
372

373 *Fig. 9: Observed radar waveforms at points close to the coast for a series of Jason cycles*
374 *(numbers on each plot refer to cycle number).*

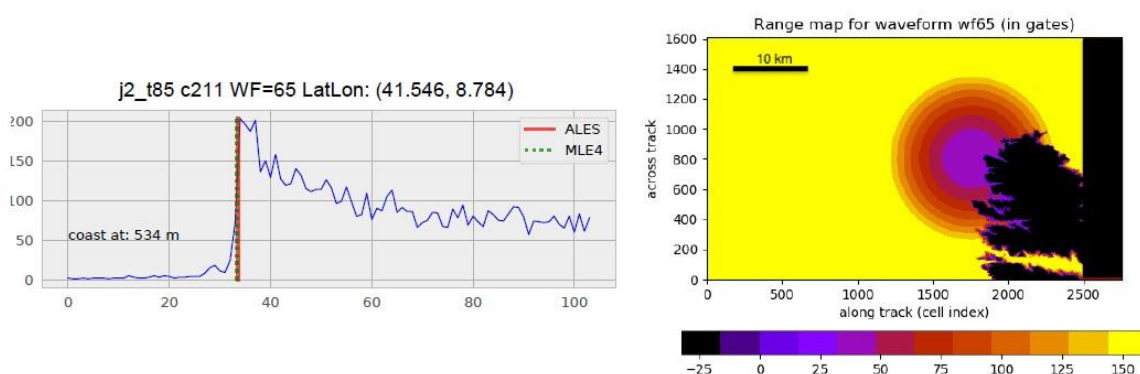
376 To investigate this further, we tried to assess the reliability of successive 20-Hz ALES-based
377 range data very close to the coast. The waveform amplitude represents the radar power as a
378

379
 380 function of time. For Jason-2, time is discretized into 104 successive ‘gates’. Knowledge of
 381 the orbit and radar footprint allows by simple geometric analysis to associate a point on
 382 ground (pixel) to a given gate. A numerical simulation has been performed for that purpose
 383 (assuming flat land) in order to produce range maps for the Jason track 85, with the goal of
 384 precisely locating the point on ground corresponding to the measured waveform. This is
 385 illustrated on Fig. 10a and Fig. 10b, showing the geographical configuration and associated
 386 radar waveforms for two range measurements located at 0.53 km and 1.4 km distance from
 387 coast. The range measurement deduced from the waveform corresponds to the center of the
 388 circle representing the radar footprint on the range map.

389
 390
 391
 392 (a)
 393



394
 395 (b)
 396



397
 398
 399 *Fig. 10: (a) Radar waveform as a function of gate number (left) and configuration of the*
 400 *radar footprint on ground (right) at 1.4 km from coast. (b) Same as (a) at 0.5 km from coast.*
 401
 402

403 Although these simulations represent an ideal case of smooth sea state and flat land, Fig.
 404 10a,b shows that even at the closest point to coast (0.5 km), the leading edge of the return

405

406 waveform still corresponds to a reflection of the radar signal on water. This suggests that it is
407 theoretically possible to retrieve valid sea level information up to 0.5 km to the coast. One
408 may argue that because the land at Senetosa has some elevation, the real radar echo is partly
409 contaminated by land reflection at distances larger than the theoretical footprint, even if there
410 is no wave. However, considering that the real waveform has a leading edge, and t h a t
411 the retracker is able to follow it, we conclude that the trends reported on successive 20-Hz
412 points are not spurious. Besides, if the retracker was corrupted by inhomogeneous backscatter
413 properties within the satellite footprint, these should be random (e.g., Passaro et al. 2014).
414 Finally, 20-Hz waveforms being independent samples, if the retracker is wrong and produces
415 spurious trends, the latter also would be random. Thus, we should not see a continuous trend
416 increase over several consecutive points.

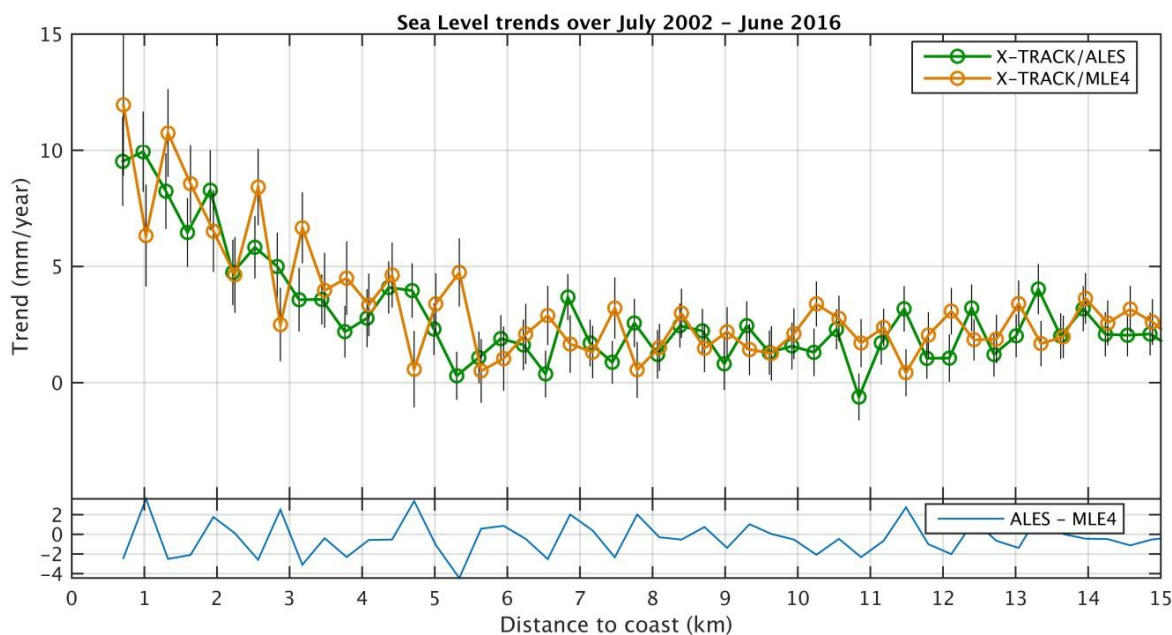
417

418 4.2.6 Comparison between ALES and MLE4 retrackers

419 Finally, we performed the same analysis (computation of sea level trends as a function of
420 distance to the coast) using SLA data computed with the classical MLE4 retracker (used for
421 the standard Geophysical Data Records production,
422 https://www.aviso.altimetry.fr/fileadmin/documents/data/tools/hdbk_tp_gdrm.pdf). MLE4-
423 based trends over the 14-year time span are shown in Fig. 11, on which are superimposed the
424 ALES-based trends, for comparison. We note that MLE4 gives noisier results than ALES,
425 especially at distances less than ~5 km to the coast, but the increase in trends in the last ~4-5
426 km to the coast is still well visible. This clearly means that the trend increase is not an artifact
427 due to the use of the ALES retracker.

428

429



430

431

432

433

434 *Fig. 11: Sea level trends as a function of distance to the coast for MLE4 (orange dots) and*
 435 *ALES (green dots)-based SLA data. Vertical bars correspond to trend errors (1-sigma). The*
 436 *light blue curve at the bottom of the panel represents the difference between ALES-based and*
 437 *MLE4-based trends.*

438

439

440

441

442

443

444

445

446

447

448

449

450

451

452

453

454

455

To summarize, from all the tests presented above, we can conclude that the increase in altimetry sea level trend observed in the last 4-5 km to the coast is not correlated with errors in the geophysical corrections, is not explained by the loss of valid data, nor the presence of spurious waveforms or by the intermission bias. Furthermore, the calculated trends are robust to change in retracker, since instead of using ALES, we also used the standard high-frequency MLE4 retracker. The corresponding time series still show the same trend behavior (although with noisier results).

5. Comparison with the sea level trend derived from tide gauges records

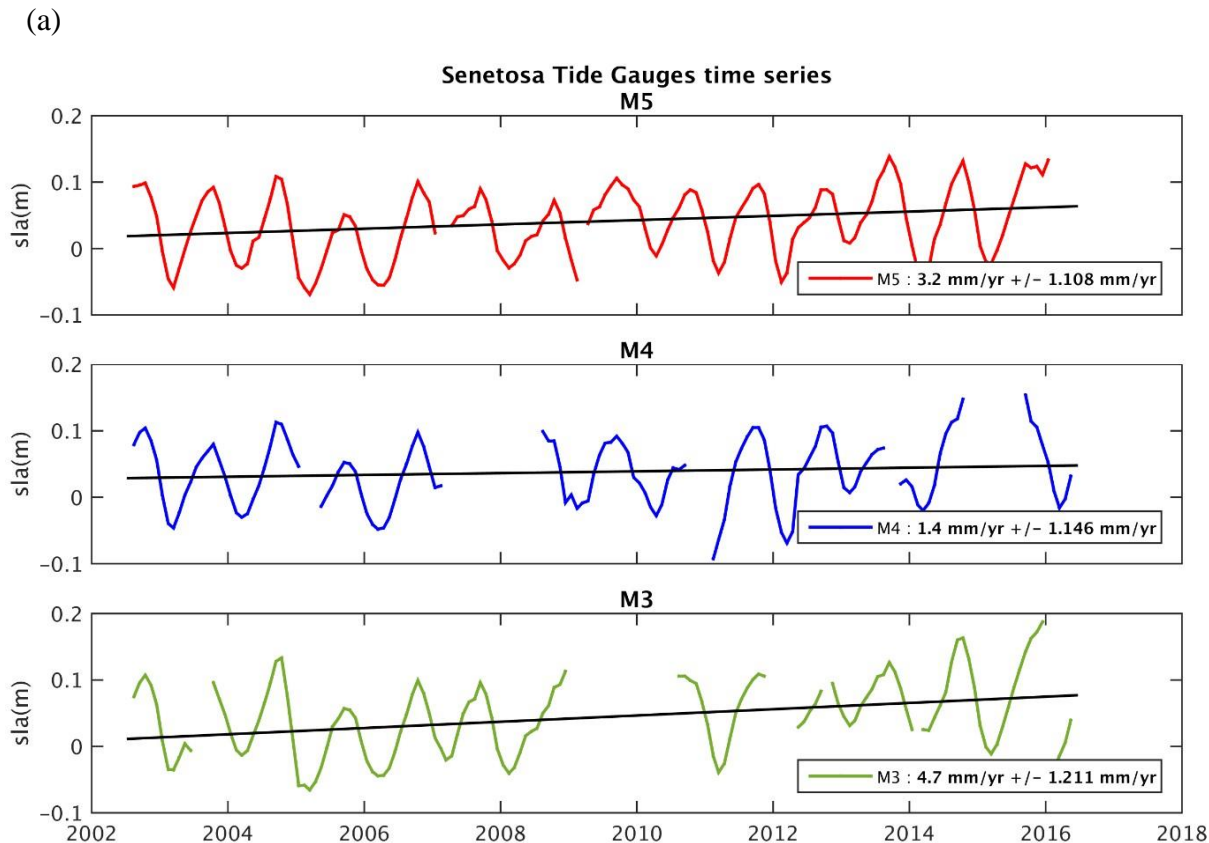
It is very classical to validate altimetry-based sea level data by comparing with tide gauge records. The availability of tide gauge records at the Senetosa site is a good opportunity to do so. Tide gauge data have been provided by the Observatoire de la Côte d'Azur (Géoazur laboratory) and downloaded from www.aviso.altimetry.fr/en/data/calval/in-situ/absolute-calibration/download-tide-gauge-data.html. The high-frequency tidal signal and the atmospheric forcing effect have been removed (using the same DAC correction as for the

456

457 altimetry data). The time series have been further smoothed on a monthly basis. The
 458 corresponding tide gauge time series over 2002-2016, for the M3, M4 and M5 tide gauges, are
 459 shown in Fig. 12a and 12b, with and without the seasonal cycles.

460

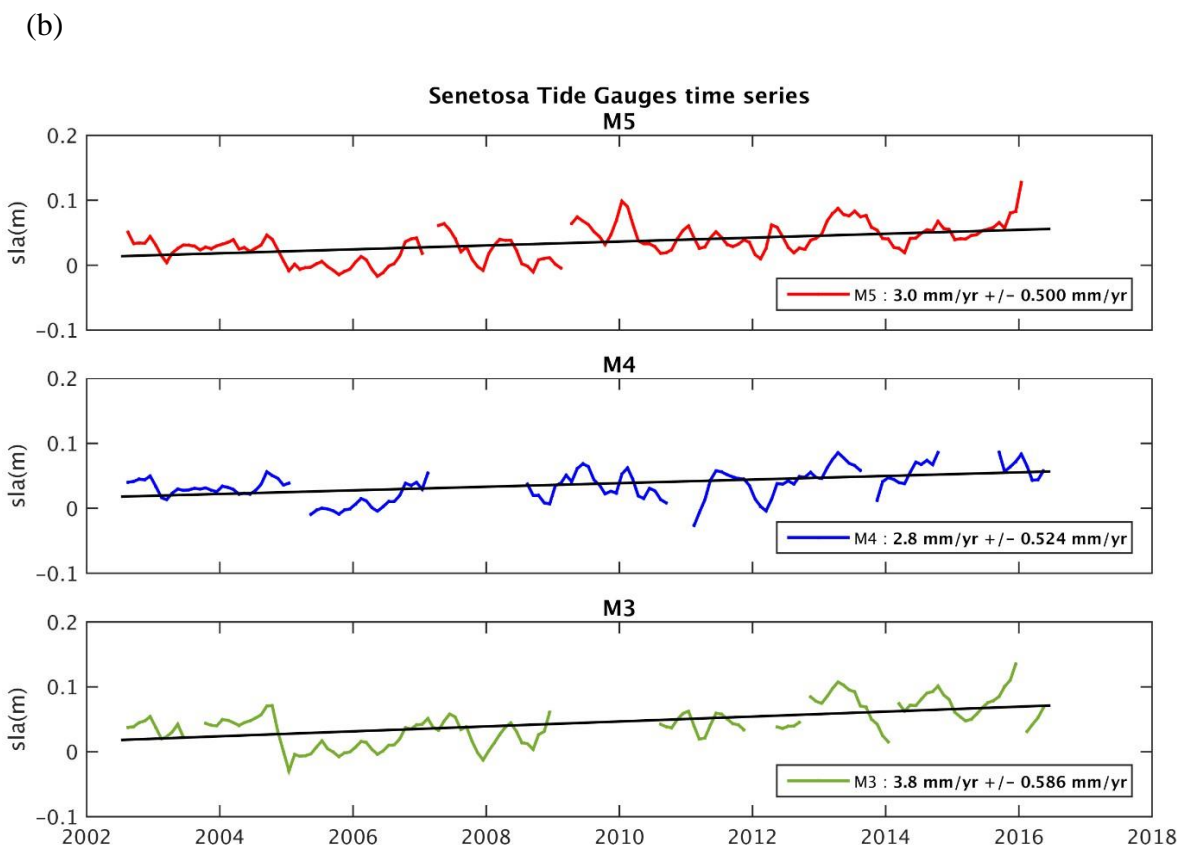
461
 462



463

464

465



466

467
468
469
470
471
472
473
474
475
476
477
478
479
480
481

Fig. 12: Sea level time series based on in situ tide gauges measurements at the M3, M4 and M5 sites over 2002-2016. (a) With the seasonal cycle. (b) Without the seasonal cycle.

From these time series, we computed linear trends over the same period as for the altimetry data. These are gathered in Table 1 for the two cases (with and without the seasonal cycle). In Bonnefond et al. (2019), it was shown that when making differences between tide gauges sea level measurements, there is no systematic trend between the tide gauge time series since 2001 (below 0.1 mm/yr), well within the trend uncertainties. The GNSS-based vertical land motion (VLM) at Senetosa (estimated in Bonnefond et al., 2019) is also shown. VLM is small at Senetosa, less than 0.3 mm/yr.

Tide Gauge	Tide gauge trend (mm/yr) (with seasonal cycles)	Tide gauge trend (mm/yr) without seasonal cycles	GNSS VLM (2003-present) (mm/yr)
M3	4.7 +/- 1.2	3.8 +/- 0.6	0.28 +/- 0.05
M4	1.4 +/- 1.1	2.8 +/- 0.5	0.28 +/- 0.05
M5	3.2 +/- 1.1	3.0 +/- 0.5	0.28 +/- 0.05

482

Table 1: Relative sea level trends (mm/yr) recorded by the M3, M4 and M5 tide gauges (estimated with and without the seasonal cycles) as well as the GNSS-based vertical land motion (mm/yr) at the Senetosa site.

486

487 The M4 time series displays several gaps over the study period. In addition, the record
488 (seasonal cycle not removed, Fig. 12a) shows a large positive anomaly in 2015, not seen by
489 M3 neither M5. M3 has also a large gap in 2009/2010, as well as other gaps 2012 and at the
490 end of the record. A suspect drop is also visible in 2005 on Fig. 12b (seasonal cycle removed).
491 Thus the M5 record seems the most reliable, even if the trends from M3 and M4 are close
492 to M5 (see Table 1). The computed (relative) sea level trend (uncorrected for the VLM) is
493 on the order of 2.8-3.8 mm/yr over the study period (seasonal cycle removed). If the GNSS
494 VLM trend is accounted for, this range becomes 3.1-4.1 mm/yr. This value is significantly
495 less than the altimetry-based sea level trends reported here in the last 4-5 km to the coast. On
496 the other hand, the tide gauge trend agree well with the altimetry-based trends reported at
497 distances greater than > 4 km from coast. While the reported altimetry-based sea level trend
498 increase may disqualify our retracked sea level data in the vicinity of the coast, in

499

500 the next section we discuss the possibility that some coastal processes affect sea level in a
501 band of a few km from the coast while being attenuated very close to the shore where the tide
502 gauges (in particular M5) are located. .

503

504 **6. Small scale coastal processes**

505 Compared to deep-ocean sea level, sea level close to the coast can be impacted by various
506 small-scales processes resulting from the morphology of the coastline, the depth of the
507 continental shelf, the presence of a river estuary, etc. (Woodworth et al., 2019). Thus coastal
508 sea level may significantly differ from open ocean sea level over a large range of temporal
509 scales. In terms of trends, the open ocean sea level essentially results from processes affecting
510 the global mean sea level (mean ocean thermal expansion, land ice melt and land water
511 storage changes) (e.g., WCRP, 2018) and the superimposed regional variability (regional
512 changes in ocean thermal expansion, atmospheric loading and fingerprints due to the solid
513 Earth response to changing ice mass loads; Stammer et al., 2013). At the coast, in addition of
514 these two contributions, local variations in other processes may cause additional small-scale
515 sea level changes at interannual to decadal time scales, such as trapped Kelvin waves,
516 upwelling/downwelling effects, eddies, wind-generated waves and swells, shelf currents, water
517 density changes related with river runoff in estuaries (see Woodworth et al., 2019 for a detailed
518 discussion on forcing factors affecting sea level changes at the coast). Note that we do not
519 discuss vertical land motion here since our objective is to understand the observed change
520 in ‘geocentric’ sea level as measured by satellite altimetry.

521 In the case of Senetosa, river runoff and trapped Kelvin waves are not supposed to affect
522 coastal sea level. Could other processes like trends in wind-generated waves and coastal
523 currents explain the slow increase in sea level trend towards the coast? These are discussed
524 below.

525

526 **6.1 Effect of waves on SLA and SSB**

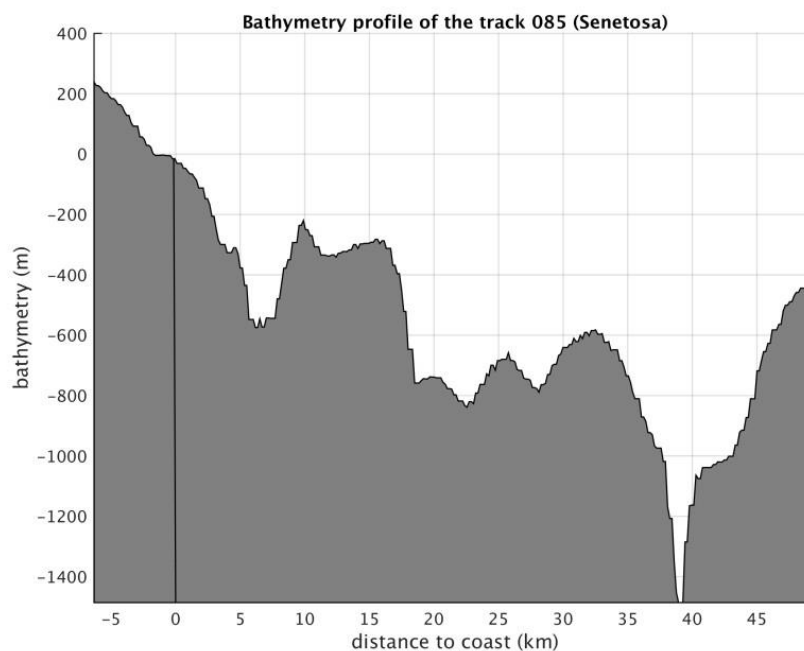
527 We first discuss the effect of waves. The contribution of wind-generated waves to coastal sea
528 level changes has been investigated in a number of recent studies (e.g., Melet et al., 2018,
529 Dodet et al., 2019). As thoroughly discussed in Dodet et al. (2019), wind-generated waves
530 have the capability to significantly change sea level variations at the coast, even at the time
531 scales of interest here. The shoaling and breaking of waves in the shelf shallow waters raises
532 the mean water level in the so-called near-shore and surf zones (last ~1 km to coast), a

533

534 process called wave set-up. Wave set-up is proportional to offshore significant wave height,
 535 and if the latter displays a temporal trend due to a trend in wind forcing, it may cause a sea
 536 level trend in the coastal zone.

537 The relationship between offshore wave height and wave set-up is known empirically only
 538 (Dodet et al., 2019). To first order, wave set-up is related to offshore SWH, wave period and
 539 beach slope. The bathymetric profile along the Jason track 85 (from 45 km offshore to coast)
 540 is shown in Fig. 13. We note an abrupt increase of more than 500 m in the last 5 km to coast,
 541 corresponding to a slope of 0.1.

542



543

544

545 *Fig. 13: Bathymetric profile (meters) along Jason track 85 from 45 km offshore to coast*

546

547

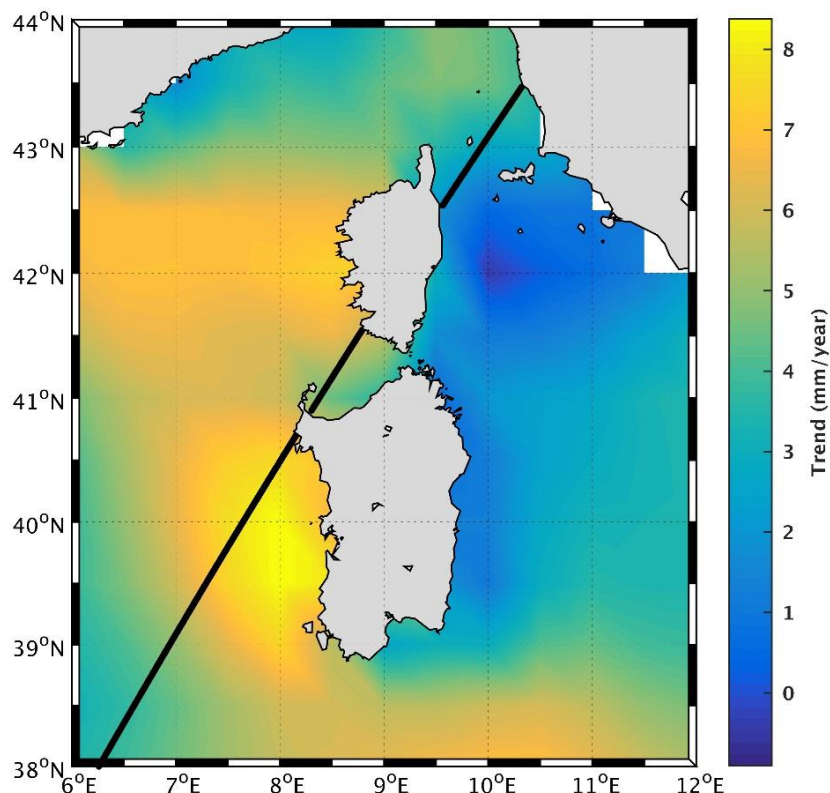
548 If the bathymetric slope near Senetosa is known, it is not the case for other parameters
 549 involved in the relationship between SWH and wave set-up. This is the case in particular for
 550 beach soil characteristics, sediment size, etc. A large variety of formulations have been
 551 proposed for this relationship, based on in situ observations collected at different coastal sites
 552 (e.g., Dodet et al., 2019). However, these are not necessarily applicable to our study case as
 553 some local beach parameters are not known. But it is generally assumed that wave set up does
 554 not exceed 20% of SWH. Thus, as a preliminary approach, we analyzed offshore SWH data
 555 only, in order to highlight their temporal variability over our study time span.

556 For that purpose we considered wave field data from the ERA5 reanalysis
 557 (<https://www.ecmwf.int/en/forecasts/datasets/reanalysis-datasets/era5>). The ERA5 reanalysis

558

559 provides gridded SWH time series at monthly interval, from 1979-present, thus covering our
 560 study period. The grid size resolution is 0.5 degree. Using this data set, we computed 2-D
 561 SWH trends over 2002-2016, shown in Fig. 14. We note high positive wave height trends
 562 west of Corsica and Sardinia over this period. Along the Jason track 85, in the vicinity of
 563 Senetosia, the trend is on the order of 5 mm/yr. Note that we also computed the wind trend using
 564 the same ERA5 reanalysis gridded data over the same period (2002-2016). The map (not shown)
 565 displays positive trends in wind south of Corsica, although with smaller amplitude than along
 566 the western coast of Sardinia, like the wave height map shown in Fig.14.

567 From the above discussion, we deduce that wave set up would not contribute by more that 1
 568 mm/yr to the coastal sea level trend. Noting in addition that wave set up would affect sea level
 569 in the close vicinity of the coast only (i.e., not over 4-5 km distance, X. Bertin, and J. Wolf,
 570 personal communications), **it is very unlikely that wave set up explains** the reported coastal
 571 sea level trend.

572
573574
575

576 *Fig. 14: Wave height trends (in mm/yr) over 2002-2016 in the western Mediterranean Sea*
 577 *(data from ERA5 reanalysis)*

578

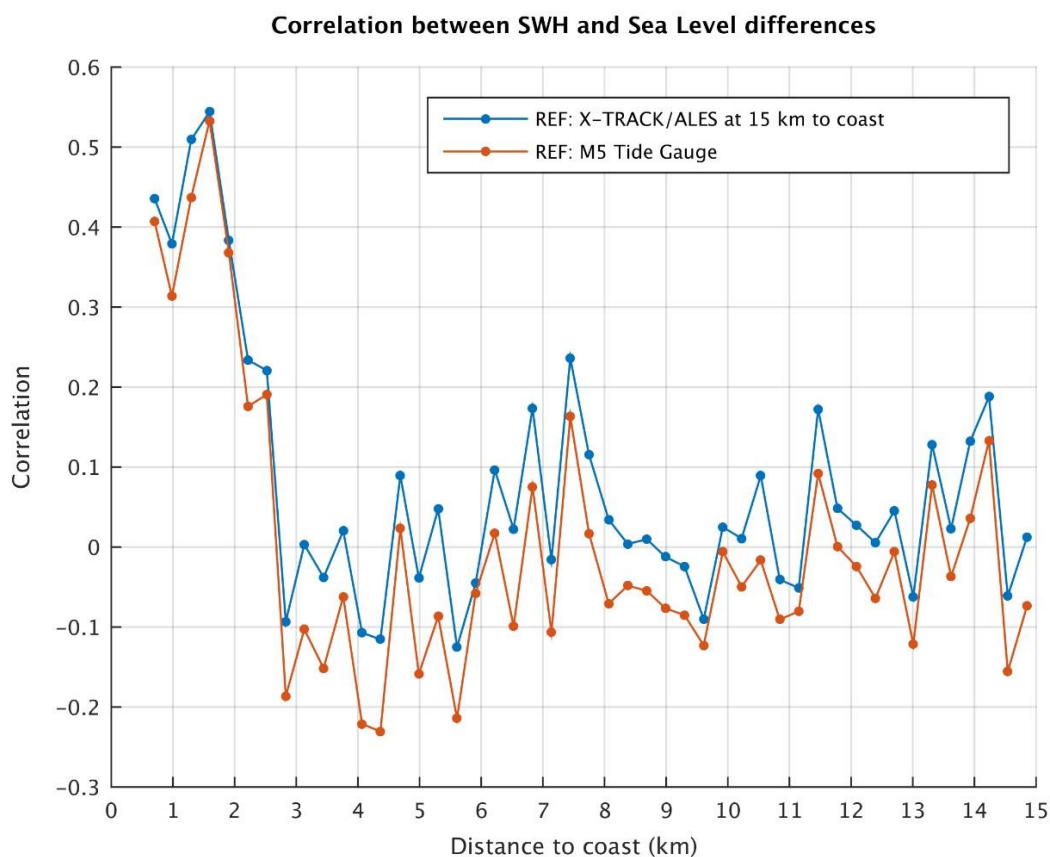
579 We further investigated the effect of waves on the ssb correction, hence on SLAs. For that
 580 purpose, we computed the correlation between wave height time series and difference in sea

581 level between each 20 Hz altimetry point and a reference altimetry point located in the

582 open ocean (chosen here at 15 km from the coast). We consider differences in sea level
 583 anomalies in order to remove the common ocean signal affecting sea level close to the
 584 coast and offshore, e.g., the global mean sea level rise and its superimposed regional
 585 variability. By computing the sea level differences between 15 km offshore and
 586 coast, the latter large-scale sea level components are removed, leaving only
 587 small-scale signals occurring very close to the coast. Data from the ERA5 grid
 588 closest to Senetosa were used (the center of the considered grid point is located at 24 km from
 589 the first valid point on the Jason track and 25 km from Senetosa). The correlation values are
 590 shown in Fig. 15 against distance to the coast. From a distance of ~3 km from the coast towards
 591 the deep sea, the correlation between wave height and sea level difference is insignificant while
 592 it clearly increases from ~3 km to the coast. This suggests that there is a link between the
 593 variations in waves and SLA variations in the 0-3 km domain close to land.

594 We performed the same analysis but now using the M5 tide gauge record as reference (the M3
 595 tide gauge record having too many data gaps). This is also shown in Fig. 15. Surprisingly, we
 596 find exactly the same behavior of the correlation coefficient, i.e., no correlation offshore
 597 (points located at distance > 3 km from coast) and an increase in correlation in the last 3 km
 598 to the coast. This now suggests that waves may affect SLA only in the domain 0-3 km from
 599 coast but that at the tide gauge site, waves have no influence. Obviously, this could be via
 600 the ssb correction applied to SLA data.

601
 602



603

604

605 *Fig. 15: Correlation between the wave height (SWH) time series (from ERA5 grid mesh close*
 606 *to Senetosa) and altimetry-based sea level difference time series between every 20 Hz point*
 607 *and a reference point. (a) The reference time series corresponds to a point located at 15 km*
 608 *from the coast. (b) The reference time series is the M5 tide gauge record.*

609

610 ~~It has been demonstrated that applying the ssb correction to altimetry data, in particular to and~~
 611 ~~even more effectively when this correction is applied at high-frequency data as in this study,~~
 612 ~~reduces the correlation between SWH and range (and, consequently, SLA) (Passaro et al.,~~
 613 ~~2018). The ssb correction is mainly a function of SWH: it removes from the range estimation~~
 614 ~~an effect that is directly proportional to the wave height. This means that if this ssb correction~~
 615 ~~is not applied, it has to be expected that the SLA record will be correlated with the SWH record.~~

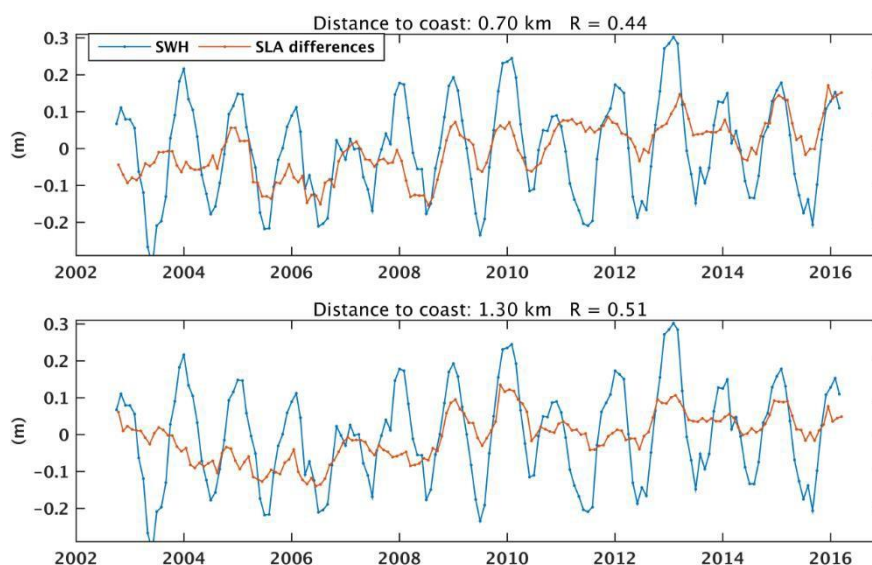
616 To illustrate this somewhat differently, Fig. 16a shows wave height time series superimposed
 617 to altimetry-based difference in SLA time series (reference point at 15 km, as in Fig. 15) for a
 618 few points located in the 0-3 km domain close to the coast and an additional point located
 619 farther from the coast. Here again, data from the ERA5 grid closest to Senetosa have been
 620 considered for the calculation. The correlation between SWH and difference SLA time series
 621 is indicated on each plot. We clearly see that it is significant only for points close to the coast.
 622 Distant offshore points do not show such a correlation. Although the correlation is
 623 dominated by the seasonal signal, Fig. 16a shows the two time series are also correlated at
 624 interannual time scales. ~~This clearly suggests that computed SLAs are impacted by waves in~~
 625 ~~the last few km to the coast on a broad range of time scales.~~

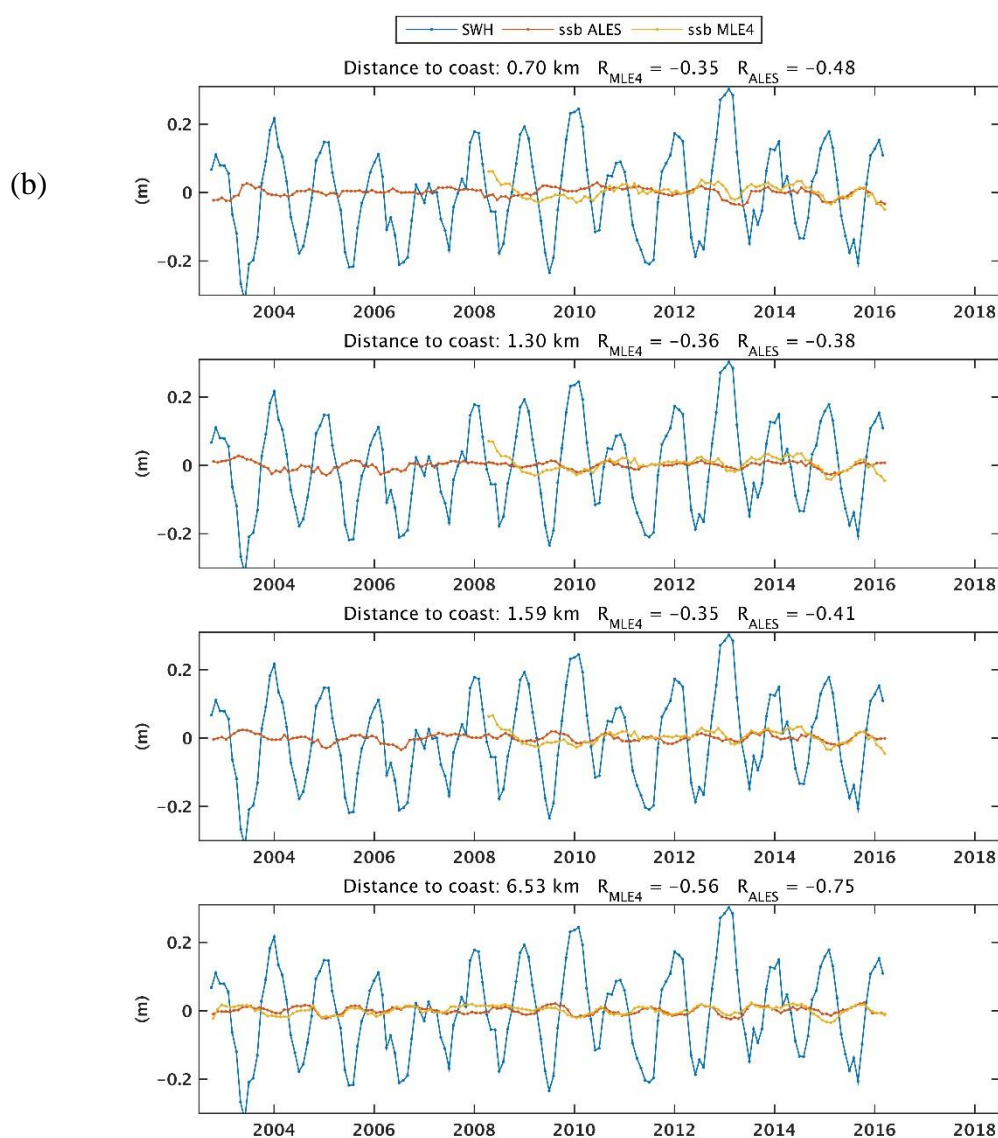
626

627 ~~We argue that when the reason is to be found in the fact that the range close to the coast is not~~
 628 ~~being properly corrected for the ssb, this which results in a correlation between ssb and with the~~
 629 ~~SWH. To verify this, we~~ repeated this correlation analysis but now using the ssb
 630 correction (from both the ALES and MLE4 retrackings) instead of the SLA
 631 differences. The corresponding figure is shown in Fig. 16b.

632

633 (a)





677 *Fig. 16: (a) Time series of ERA5-based wave height time series (blue curve) and of altimetry-*
 678 *based SLA differences (orange curve) between 20 Hz points at different distances from coast*
 679 *(indicated on each plot) and a reference point (located at 15 km). (b) same as (a) but using*
 680 *ALES ssb instead of SLA differences. On Fig. 16b, MLE4 ssb are also shown for the Jason-2*
 681 *time span (yellow curve). R is the correlation coefficient.*

682 As expected, ssb is correlated with SWH wave height away from the coast, but the correlation
 683 decreases in the last few km to the coast, suggesting that the relationship used to express
 684 the link between ssb and SWH is less adapted in the coastal domain than in the open sea,
 685 possibly either because of change of wave properties (which makes the common-ssb model
 686 invalid) or because of a wrong estimation of SWH very close to the coast. This is also illustrated
 687 in Fig. 17 that shows the correlation between ssb and SWH against to as a function of distance
 688 to the coast (for both ALES ssb and MLE4 ssb). Between 1 km

689
690
691
692

and 4 km, the correlation between SWH and ssb decreases. It is worth noting however that the correlation but remains higher for ALES ssb than for MLE4 ssb.

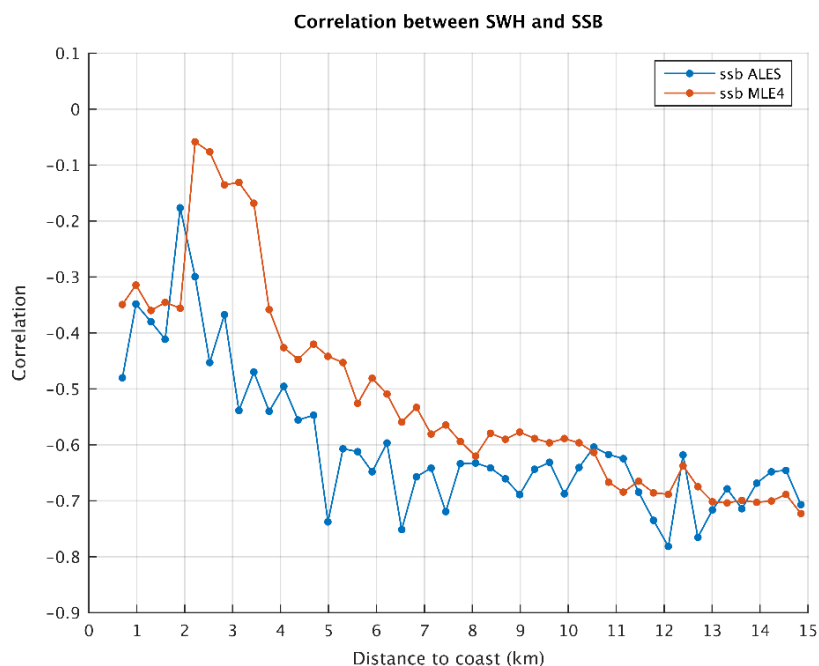
693
694

Fig. 17: Correlation between significant wave height (SWH) time series and ssb time series between every 20 Hz point and a reference point.

697

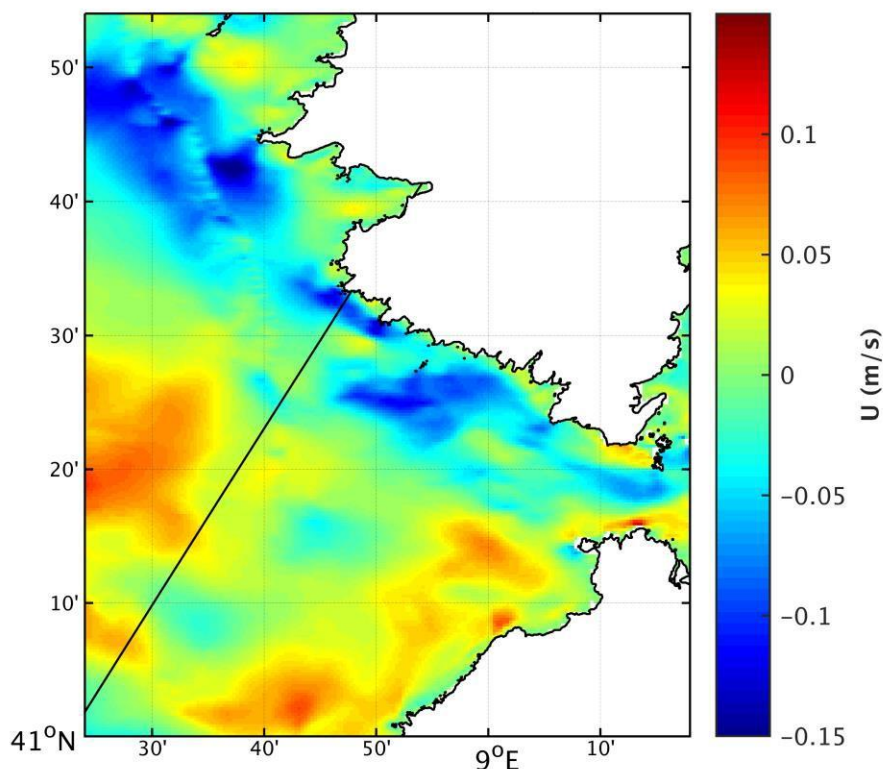
We conclude from these tests, that the correlation between SLA and wave height at 20 Hz points close to the coast is very likely due to imperfect ssb correction. Thus we can now exclude any direct effect of waves (e.g., trend in wave set-up) as a candidate to explain the SLA trend increase close to the coast. Are the reported SLA trends in the last few km to the coast due to inadequate formulation of the relationship between SWH and ssb as the satellite approaches the coast remains so far an open question. While we cannot exclude that the ssb correction is imperfect close to the coast, it seems unlikely that it would produce such large trends as those observed in the SLAs.

706

707 6.2. Effect of coastal currents and comparison with an ocean model

708 In this section we briefly address the effect of coastal currents on the SLAs. There are only
709 few published studies on the circulation in the Senetosa region (e.g., Bruschi et al., 1981,
710 Manzena et al., 1985, Cucco et al., 2012, Gerigny et al., 2015, Sciascia et al., 2019). These
711 indicate that the dominant characteristics of the circulation in the Corsica channel (Bonifacio
712 Straits) is a flow predominantly directed northward from the Tyrrhenian Sea to the Ligurian

713
 714 Sea and that the water motion is mainly wind-driven. The study by Gerigny et al. (2015)
 715 based on in situ measurements collected during a cruise in 2012 and use of a high-resolution
 716 regional hydrodynamic model (MARS3D) shows that the circulation is mostly wind-driven,
 717 **forced by westerly winds half of the year and strong easterly winds in winter, generating strong**
 718 **local currents and mesoscale structures in the western part of the channel.** We have
 719 downloaded the currents data generated by the MARS3D model, a coastal hydrodynamical
 720 model developed by IFREMER (Institut Français de Recherche pour l'Exploitation de la
 721 Mer; Lazure and Dumas 2008). There is a high-resolution (400 m) version available for the
 722 Corsica region, for the years 2014 to present
 723 (<http://www.ifremer.fr/docmars/html/doc.basic.intro.html>). The model does not assimilate
 724 altimetry data nor any other type of data. Because this dataset has only 2.5 years of overlap with
 725 our study period, we cannot compute trends. However, to gain some insight on the circulation
 726 configuration, we examined the currents pattern over the year 2014. In agreement with the
 727 literature, we observed a strong zonal current during the winter months close to Senetosa. An
 728 example of the zonal component of the barotropic current south of Corsica is shown in Fig.18
 729 for January 2014. We note a clear westward current along the Senetosa coast starting **at ~4 km**
 730 **from the coast.** It is also worth noting that it does not extend to the shoreline, thus may not
 731 influence tide gauge measurements.
 732



733

734

735 *Fig.18: Barotropic current (zonal component) for January 2014 based on the MARS3D*
 736 *hydrographic model. Blue color means westward current. The Jason track (black line) crosses*
 737 *this current at 4 km from the coast.*

738

739 We interpolated these current data (for January 2014) along the Jason track. This is shown in
 740 Fig.19 against distance to the coast. The current intensity is close to zero at distances >5km from
 741 the coast. In the last 5 km to the coast, there is a steep intensity increase, exactly over the same
 742 distance range as the SLA trend increase. Since the model resolution is ~400m, i.e., about the
 743 same resolution as the 20 Hz along-track SLAs, we find this result highly promising.

744

745

746

747

748

749

750

751

752

753

754

755

756

757

758

759

760

761

762

763

764

765

766

767

768

769

770

771

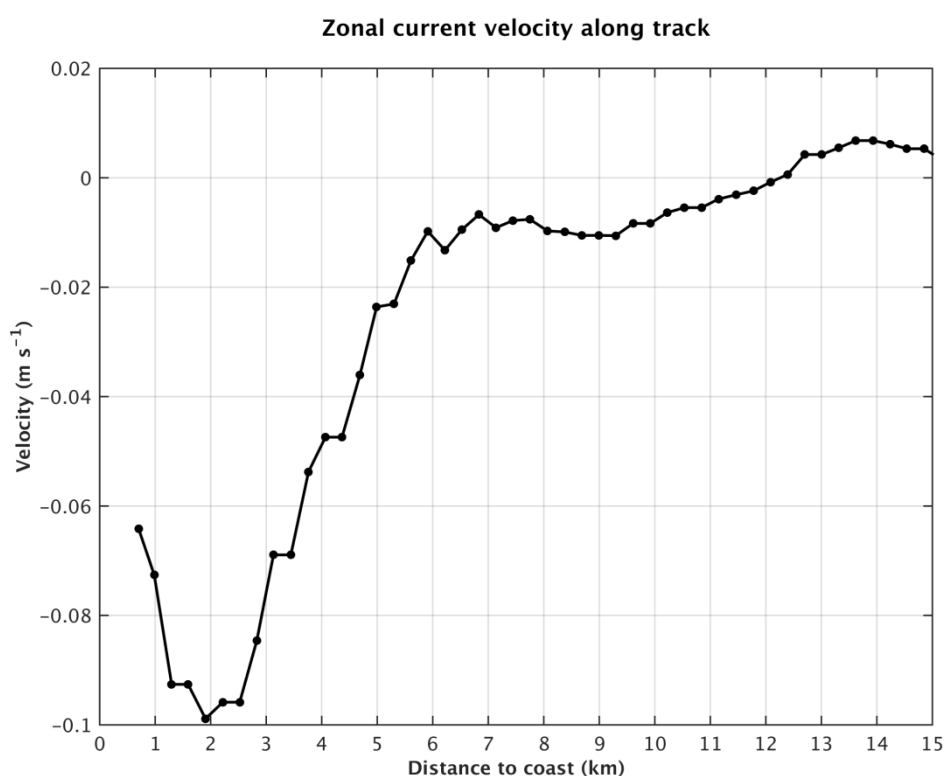
772

773

774

775

776



769 *Fig.19: Barotropic current (zonal component) for January 2014 based on the MARS3D*
 770 *hydrographic model interpolated along the Jason track, as a function of distance to the coast.*
 771 *Negative values mean westward current.*

772

773 Of course, we cannot extrapolate backward in time nor offer any solid conclusion so far. But we
 774 cannot exclude that the observed sea level trend increase is linked to an increase in intensity of
 775 this winter current during our study period. This obviously will need much deeper investigation,
 776 at least over the time span of availability of the model data.

777

778 **7. Conclusion**

779 In this study, we have investigated the differences between coastal and deep ocean sea level
780 changes at the Senetosa site, using new ALES-based retracked sea level data from the Jason-1
781 and Jason-2 missions. We indeed observe a slow increase in sea level trend at short ($< \sim 4\text{-}5$
782 km) distance from the coast compared to offshore. A series of test shows that this behavior
783 does not result from artifacts due to spurious trends in the geophysical corrections applied to
784 the altimetry data, decreasing percentage of valid data, or errors in the intermission bias nor
785 errors in range estimates due to distorted radar waveforms.

786 While the paper was in review, an update of the results presented above has been recently
787 performed extending the SLA time series with Jason-3 data up to June 2018 (coastal trends based
788 on Jason-1, 2 and 3 over 2002-2018 at several hundreds of coastal sites located in six different
789 regions worldwide are presented elsewhere; The Climate change Initiative Coastal Sea Level
790 Team, 2020). Although the coastal trends within the 2-3 km to the coast are slightly lower than
791 those reported above, exactly the same behavior is found, as shown in Fig.20 that compares
792 coastal trends over 2002-2016 and 2002-2018. Thus, the trend increase close to the coast
793 observed at Senetosa is not due to the limited length of the time series, although its amplitude
794 decreases as the record length increases. Similarly, the geophysical correction trends present the
795 same behavior over both time spans. It is worth mentioning that in the extended study (2002-
796 2018), among the 429 studied coastal sites, coastal trends do not in general differ from open
797 ocean trends (within ± 1 mm/yr), except at a few sites (The Climate Change Initiative Coastal
798 Sea Level Team, 2020), Senetosa is one of them. This is why we made a focus on that particular
799 site.

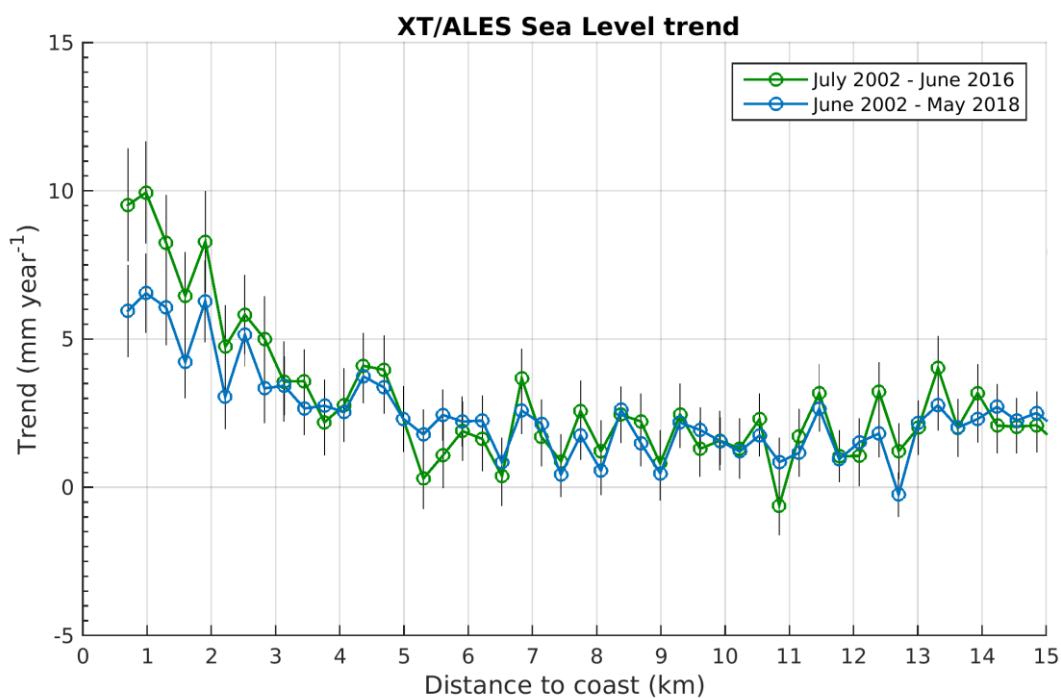
800

801

802

803

804



805 *Fig.20. Altimetry-based sea level trends at Senetosa, over two periods: (1) July 2002-June*
 806 *2016, green curve and (2) June 2002-May 2018, blue curve. Black vertical bars*
 807 *correspond to trend uncertainties.*

808

809 Among the physical mechanisms able to explain the coastal trend increase in the study region,
 810 we have first explored waves, then currents. We investigated the wave effect on sea level
 811 along the Jason track and found that wave set up has a too small magnitude and is localized
 812 too close to the shore to explain the observed continuous SLA trend increase in the last 4-5
 813 km to the coast. On the other hand, the correlation reported between altimetry-based SLAs
 814 and SWH very likely results from the imperfect ssb correction applied to the data.
 815 Nevertheless, if less accurate in the coast vicinity, the ssb trend seems unable to explain the
 816 reported SLA trend increase. We next investigated the effect of coastal currents. Using the
 817 MARS3D high resolution model developed by IFREMER for coastal studies, we noted the
 818 presence of a winter current along the Senetosa coastline. Projection of this current along the
 819 Jason track (for January 2014) shows a step increase in intensity over exactly the same
 820 distance to the coast as the SLA trend increase. This may be an indication of a current-related
 821 origin. More studies are definitely needed to confirm the results presented here. However, if
 822 further investigations confirm the effect of currents, it will be a demonstration that small-
 823 scale processes acting in the vicinity of the coast may have the capability to make coastal sea
 824 level changes drastically different from what we measure offshore with classical altimetry.

825

826

827

828 Acknowledgements

829
830 This study is a contribution to the ESA Climate Change Initiative (CCI+) Sea Level project.
831 Yvan Gouzenes is supported by an engineer grant in the context of this project (ESA SL_cci+
832 contract number 4000126561/19/I-NB). We thank a number of colleagues for very fruitful
833 discussions on the effect of waves on tide gauges and coastal sea level, in particular (by
834 alphabetic order) Angel Amores, Xavier Bertin, Svetlana Jevrejeva, Goneri Le Cozannet,
835 Marta Marcos, Judy Wolf and Phil Woodworth. **We also thank two anonymous reviewers and
836 the Editor for their comments and suggestions to improve the manuscript.**

837

838

839 Data availability

840 **The coastal sea level data analyzed in this study are available from the Nature Scientific Data**
841 **article (The Climate change Initiative Coastal Sea Level Team, 2020). The ERA wave field**
842 **data from the ERA5 reanalysis are available from the following web site:**
843 **<https://www.ecmwf.int/en/forecasts/datasets/reanalysis-datasets/era5>.**
844 **The MARS3D model can be downloaded from the web site:**
845 **<http://www.ifremer.fr/docmars/html/doc.basic.intro.html>**

846
847848 **References**

849

850 Ablain M., Legeais J.F., Prandi P., et al., 2017. Altimetry-based sea level, global and regional
851 [scales](#).852 *Surveys in Geophysics*, 38, 7-31, <https://doi.org/10.1007/s10712-016-9389-8>.

853

854 Almar, R., E. Kestenare, J. Reyns, J. et al., 2015. Response of the Bight of Benin (Gulf of
855 Guinea, West Africa) coastline to anthropogenic and natural forcing, Part1: Wave climate
856 variability and impacts on the longshore sediment transport, *Continental Shelf Research*, 110,
857 48-59, <https://doi.org/10.1016/j.csr.2015.09.020>.858 Birol F. and C. Delebecque, 2014. Using high sampling rate (10/20 Hz) altimeter data for the
859 observation of coastal surface currents: A case study over the northwestern Mediterranean
860 Sea, *J. Mar. Syst.*, <https://doi.org/10.1016/j.jmarsys.2013.07.009>.

861

862 Birol F., N.X Fuller, F. Lyard, et al., 2017. Coastal applications from nadir altimetry: example
863 of the X-TRACK regional products. *Advances in Space Research*, 59, 936-953,
864 <https://doi.org/10.1016/j.asr.2016.11.005>.

865

866 Bruschi A., Buffoni G., Elliott A.J., Manzella G., 1981. A numerical investigation of the
867 wind-driven circulation in the Archipelago of La Maddalena, *Oceanol. Acta*, 4, 3, 289-295.

868

869 Bonnefond, P., Exertier, P., Laurain, O., Ménard, Y., Orsoni, A., Jan, G., Jeansou, E., 2003a,
870 Absolute calibration of Jason-1and TOPEX/Poseidon altimeters in Corsica, in: Special Issue
871 on Jason-1 Calibration/ Validation, Part 1. *Mar. Geod.* 26(3-4), pp. 261-284,
872 <https://doi.org/10.1080/714044521>.

873

874 Bonnefond, P., Exertier, P., Laurain, O., Ménard, Y., Orsoni, A., Jeansou, E., Haines, B.J.,
875 Kubitschek, D.G., Born, G.H. Leveling sea surface using a GPS catamaran, 2003b, in:
876 Special Issue on Jason-1 Calibration/ Validation, Part 1. *Mar. Geod.* 26(3-4), 319-334,
877 <https://doi.org/10.1080/714044524>.

878

879 Bonnefond, P., Exertier, P., Laurain, O., Jan, G., 2010, Absolute calibration of Jason-1 and
880 Jason-2 altimeters in Corsica during the formation flight phase, in: Special Issue on Jason-2
881 Calibration/Validation, Part 1. *Mar. Geod.* 33(S1), 80-90,
882 <https://doi.org/10.1080/01490419.2010>.

883

884 Bonnefond, P., B. Haines and C. Watson. In Situ Calibration and Validation: A Link from
885 Coastal to Open-ocean altimetry, 2011, in Coastal Altimetry, chapter 11, pp 259-296, edited
886 by S. Vignudelli, A. Kostianoy, P. Cipollini, J. Benveniste, Springer, ISBN: 978-3-642-
887 12795-3. https://doi.org/10.1007/978-3-642-12796-0_11

888

889 Bonnefond, P., Exertier, P., Laurain, O., Guinle, ., F m nias, ., 201 , Corsica: A 20-Yr
890 Multi-Mission Absolute Altimeter Calibration Site, *Advances in Space Research*, Special
891 Issue « 25 Years of Progress in Radar Altimetry », <https://doi.org/10.1016/j.asr.2019.09.049>.

892

893 Carrere, L. and Lyard, F. 2003. Modeling the barotropic response of the global ocean to
894 atmospheric wind and pressure forcing- comparisons with observations. *J. Geophys. Res.* 30 (6),
895 1275. <http://dx.doi.org/10.1029/2002GL016473>.

896

897 Carrere L., Lyard, F., Cancet, M., Guillot, A., Roblou, L., 2012. FES2012: A new global tidal
898 model taking taking advantage of nearly 20 years of altimetry, Proceedings of meeting "20
899 Years of Altimetry", Venice 2012.

- 900
901 Cartwright, D. E. and R. J. Taylor, 1971. New computations of the tide-generating potential,
902 *Geophys. J. R. Astron. Soc.*, 23, 45-74.
903
- 904 Cartwright, D. E. and Edden, A. C., 1973. Corrected Tables of Tidal Harmonics. *Geophysical Journal*
905 *of the Royal Astronomical Society*, 33: 253-264. doi:10.1111/j.1365-246X.1973.tb03420.x.
906
- 907 Church, J. A. et al., 2013: Sea Level Change. In: Climate Change 2013: The Physical Science
908 Basis. Contribution of Working Group I to the Fifth Assessment Report of the
909 Intergovernmental Panel on Climate Change [Stocker, T. F., D. Qin, G. K. Plattner, M.
910 Tignor, S. K. Allen, J. Boschung, A. Nauels, Y. Xia, V. Bex and P. M. Midgley (eds.)].

- 911 Cambridge University Press, Cambridge, United Kingdom and New York, NY, USA, 1137-
912 1216.
- 913 Cipollini P., J. Benveniste, F. Birol, et al., 2018. Satellite altimetry in coastal regions. In
914 'Satellite altimetry over the oceans and land surfaces', Stammer & Cazenave Edts, CRC
915 Press, Taylor and Francis Group, Boca Raton, London, New York, pp 343-373,
916 <https://doi.org/10.1201/9781315151779-11>
- 917
918 Climate Change Initiative Coastal Sea level Team (The), 2020, A database of coastal sea level
919 anomalies and associated trends from satellite altimetry from 2002 to 2018, in revision, *Nature*
920 *Scientific Data*.
- 921
922 Cucco A et al., 2012, A high-resolution real-time forecasting system for predicting the fate of
923 oil spills in the Strait of Bonifacio (western Mediterranean Sea), *Marine Pollution Bulletin*,
924 64, 1186-1200, doi:10.1016/j.marpolbul.2012.03.019.
- 925
926 Dieng, H., A. Cazenave, B. Meyssignac and M. Ablain, 2017: New estimate of the current
927 rate of sea level rise from a sea level budget approach. *Geophysical Research Letters*, 44 (8),
928 3744-3751, <https://doi.org/10.1002/2017GL073308>.
- 929
930 Dodet G., Melet A., Arduin F., Bertin X ;, Idier D. and Almar R., 2019. The contribution of
931 wind-generated waves to coastal sea level changes, *Surveys in Geophysics*, 40, 1563-1601,
932 <https://doi.org/10.1007/s10712-019-09557-5>.
- 933
934 Durand F., Piecuch C., Cirano M. et al., 2019. Impact of continental freshwater runoff on
935 coastal sea level, *Surveys in Geophysics*, 40:1437–1466, [https://doi.org/10.1007/s10712-019-](https://doi.org/10.1007/s10712-019-09536-w)
936 09536-w.
- 937
938 Fernandes, M.J., Lazaro, C., Ablain, M., Pires, N., 2015. Improved wet path delays for all ESA
939 and reference altimetric missions. *Remote Sens. Environ.* 169, 50–74,
940 <http://dx.doi.org/10.1016/j.rse.2015.07.023>.
- 941
942 Gerigny O., Coudray S., Lapucci C. , Tomasino C., Bisgambiglia P.A., Galgani F., 2015,
943 Small-scale variability of the current in the Strait of Bonifacio, *Ocean Dynamics*, 65, 8, 1165-
944 1182, <http://dx.doi.org/10.1007/s10236-015-0863-5>.
- 945
946 Jebri, F., Birol, F., Zakardjian, B., Bouffard, J., Sammari, C., 2016. Exploiting coastal altimetry
947 to improve the surface circulation scheme over the Central Mediterranean Sea: circulation In
948 The Central Mediterranean. *J. Geophys. Res. Oceans* 121 (7), 4888–4909. [http://](http://dx.doi.org/10.1002/2016JC011961)
949 dx.doi.org/10.1002/2016JC011961.
- 950
951 Lazure P and Dumas F, 2008, An external–internal mode coupling for a 3D hydrodynamical
952 model for applications at regional scale (MARS), *Advances in Water Resources*, 31:233-250,
953 doi:10.1016/j.advwatres.2007.06.010.
- 954
955 Legeais J.F., Ablain M., Zawadzki L. et al., 2018. An improved and homogeneous altimeter
956 sea level record from the ESA Climate Change Initiative, *Earth Syst. Sci. Data*, 10, 281-301,
957 <https://doi.org/10.5194/essd-10-281-2018>.
- 958
959 Léger F., F. Birol, F. Niño, M. Passaro, F. Marti and A. Cazenave, 2019, "X-Track/Ales
960 Regional Altimeter Product for Coastal Application: Toward a New Multi-Mission Altimetry
961 Product at High Resolution," IGARSS 2019 - 2019 IEEE International Geoscience and Remote
962 Sensing Symposium, Yokohama, Japan, 8271-8274,
<https://doi.org/10.1109/IGARSS.2019.8900422>.

- 963
964 Manzella G.M.R., 1985, Fluxes across the Corsica Channel and coastal circulation in the East
965 Ligurian Sea, North-Western Mediterranean, *Oceanol. Acta*, 8, 1, 29-35.
966
967 Marti F., Cazenave A., Birol F., Passaro, M. Leger F., Nino F., Almar R., Benveniste J. and
968 Legeais J.F., 2019, Altimetry-based sea level trends along the coasts of western Africa, *Adv.*
969 *in Space Res.*, published online 24 May2019, <https://doi.org/10.1016/j.asr.2019.05.033>,.

970

971 Melet, A., Almar, R. and Meyssignac, B., 2016. What dominates sea level at the coast: a
 972 case study for the Gulf of Guinea. *Ocean Dyn.* 66, 623–636,
 973 <https://doi.org/10.1007/s10236-016-0942-2>.

974 Melet A., Meyssignac B. Almar R. et al., 2018. Under-estimated wave contribution to
 975 coastal sea-level rise, *Nature Climate Change*, 8, 234–239, [https://doi.org/10.1007/s10236-](https://doi.org/10.1007/s10236-016-0942-2)
 976 [016-0942-2](https://doi.org/10.1007/s10236-016-0942-2).

977 Nerem, R. S. et al., 2018: Climate-change–driven accelerated sea-level rise detected in the
 978 altimeter era. *Proceedings of the National Academy of Sciences*,
 979 <https://doi.org/10.1073/pnas.1717312115>.
 980

981 Passaro M., Cipollini P., Vignudelli S. et al., 2014. ALES: A multi-mission subwaveform
 982 retracker for coastal and open ocean altimetry. *Remote Sensing of Environment* 145, 173-189,
 983 <https://doi.org/10.1016/j.rse.2014.02.008>.

984 Passaro M., Cipollini P., Benveniste J., 2015, Annual sea level variability of the coastal
 985 ocean: the Baltic Sea-North Sea transition zone. *J Geophys Res Oceans* 120(4):3061–3078,
 986 <https://doi.org/10.1002/2014JC010510>.

987 Passaro M., Zulfikar Adlan N. and Quartly G.D., 2018. Improving the precision of sea level
 988 data from satellite altimetry with high-frequency and regional sea state bias corrections.
 989 *Remote Sensing of Environment*, 245-254, <https://doi.org/10.1016/j.rse.2018.09.007>.

990 Piecuch C.G., Bittermann K., Kemp A.C. et al., (2018). River-discharge effects on United
 991 States Atlantic and Gulf coast sea-level changes, *PNAS*, vol. 115, no. 30, 7729–7734,
 992 <https://doi.org/10.1073/pnas.1805428115>.

993
 994 Sciascia R., Magaldi M. and Vetrano A., 2019, Current reversal and associated variability
 995 within the Corsica Channel: The 2004 case study, *Deep-Sea Research Part I*, 144, 39-51.
 996

997 SROCC 2019: IPCC Special Report on the Ocean and Cryosphere in a Changing Climate
 998 [H.-O. Pörtner, D.C. Roberts, V. Masson-Delmotte, P. Zhai, M. Tignor, E. Poloczanska, K.
 999 Mintenbeck, A. Alegría, M. Nicolai, A. Okem, J. Petzold, B. Rama, N.M. Weyer (eds.)].et al.].
 1000 In press.

1001 Stammer D, Cazenave A, Ponte RM, Tamisiea ME (2013) Causes for contemporary regional
 1002 sea level changes. *Annu Rev Mar Sci.* <http://doi.org/10.1146/annurev-marine-121211-172406>
 1003

1004
 1005 Wahr, J.M., 1985. Deformation Induced by Polar Motion. *J. Geophys. Res.*, 90 (B11), 9363–
 1006 9368.

1007
 1008 Vignudelli S. , A. G. Kostianoy, P. Cipollini, and J. Benveniste (Eds.), 2011, Coastal
 1009 Altimetry, Springer, Berlin, <https://doi.org/10.1007/978-3-642-12796-0>.

1010 The WCRP Global Sea Level Budget Group (2018). Global sea level budget, 1993-present.
 1011 *Earth Syst. Sci. Data*, 10, 1551–1590, <http://doi.org/10.5194/essd-10-1551-2018>.

1012 Woodworth P., Melet A., Marcos M. et al., 2019. Forcing Factors Causing Sea Level Changes
 1013 at the Coast, *Surveys in Geophysics*, <https://doi.org/10.1007/s10712-019-09531-1>.

1014

1015 Wöppelmann, G., and M. Marcos (2016), Vertical land motion as a key to understanding sea
1016 level change and variability, *Rev. Geophys.*, 54, 64–92,
1017 <https://doi.org/10.1002/2015RG000502>.